Space Weather Research using a desktop/laptop computer and a free online database (Researching Palapa's space environment)

Simon Wing

The Johns Hopkins University
Applied Physics Laboratory

outline

1. Motivation
2. Spacecraft charging
3. Researching geosynchronous orbit space environment
4. A space weather tool: neural networks
5. Summary

1. Motivation

Geosynchronous orbit

- Indonesia has owned Palapa series satellites since the mid 1970s, for almost 4 decades
- All Palapa satellites were/are located at geosynchronous orbit
- Geosynchronous orbit is an attractive place to park satellites
  - stable orbit – save fuel
  - fixed geographical coverage

PALAPA-B Satellites

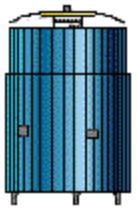

PALAPA-C

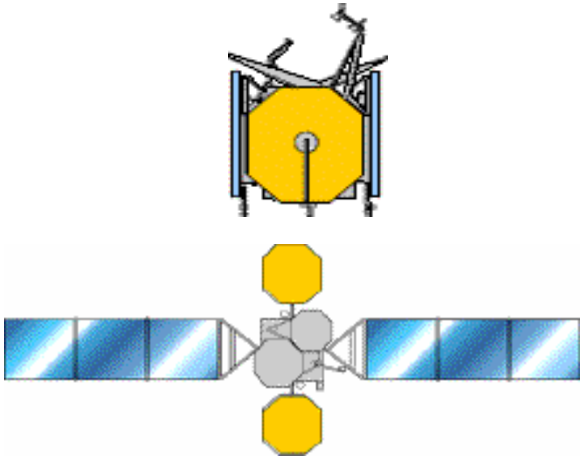

launched in 1996

PALAPA-C Coverage

Geosynchronous orbit

- Indonesia has owned Palapa series satellites since the mid 1970s, for almost 4 decades
- All Palapa satellites were/are located at geosynchronous orbit
- Geosynchronous orbit is an attractive place to park satellites
  - stable orbit – save fuel
  - fixed geographical coverage
  - **space weather risk: spacecraft charging, noise, etc.**

PALAPA-B Satellites

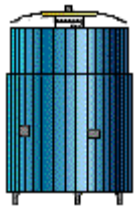

2. Spacecraft charging

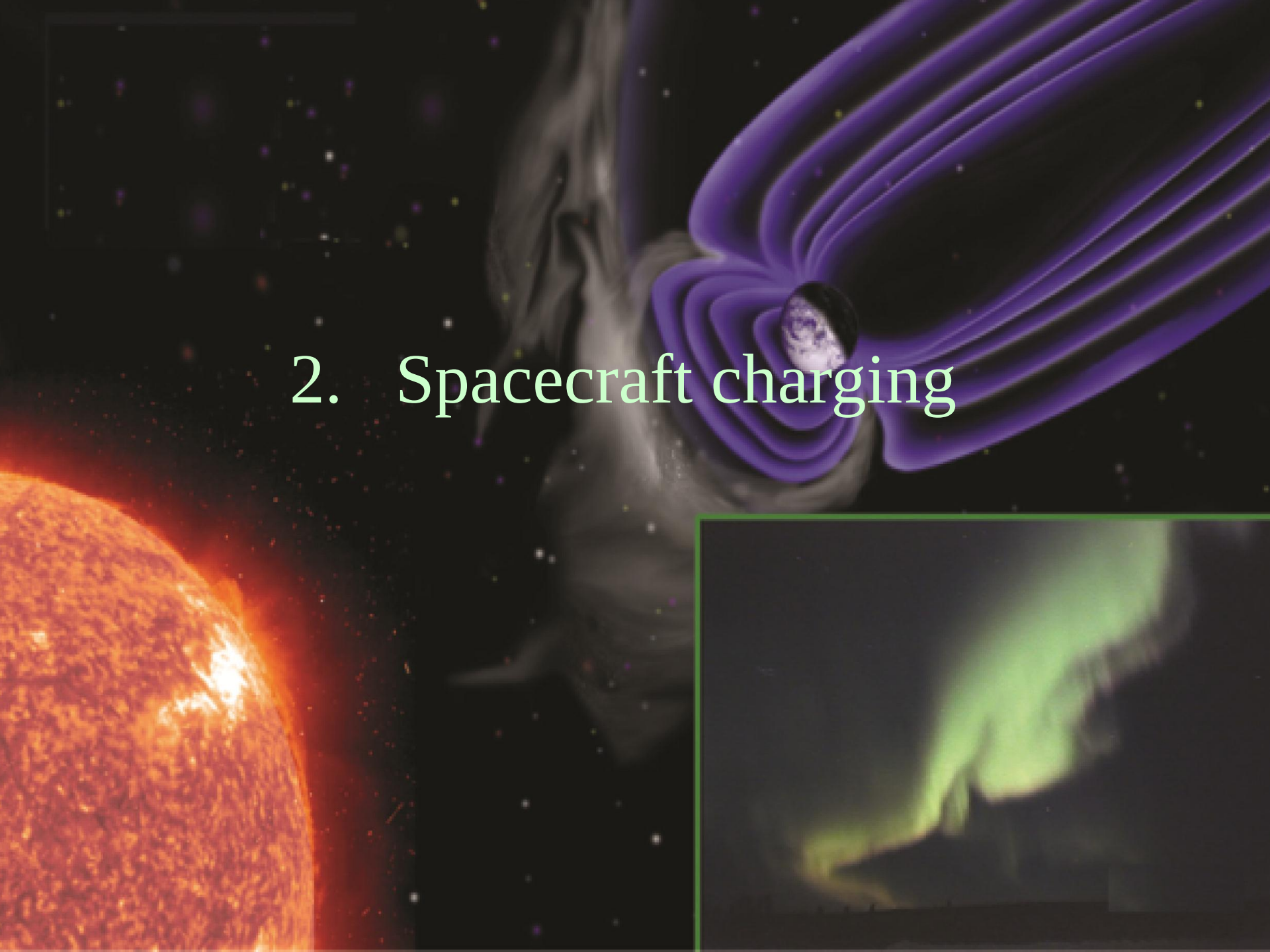

Space weather effect: Spacecraft charging

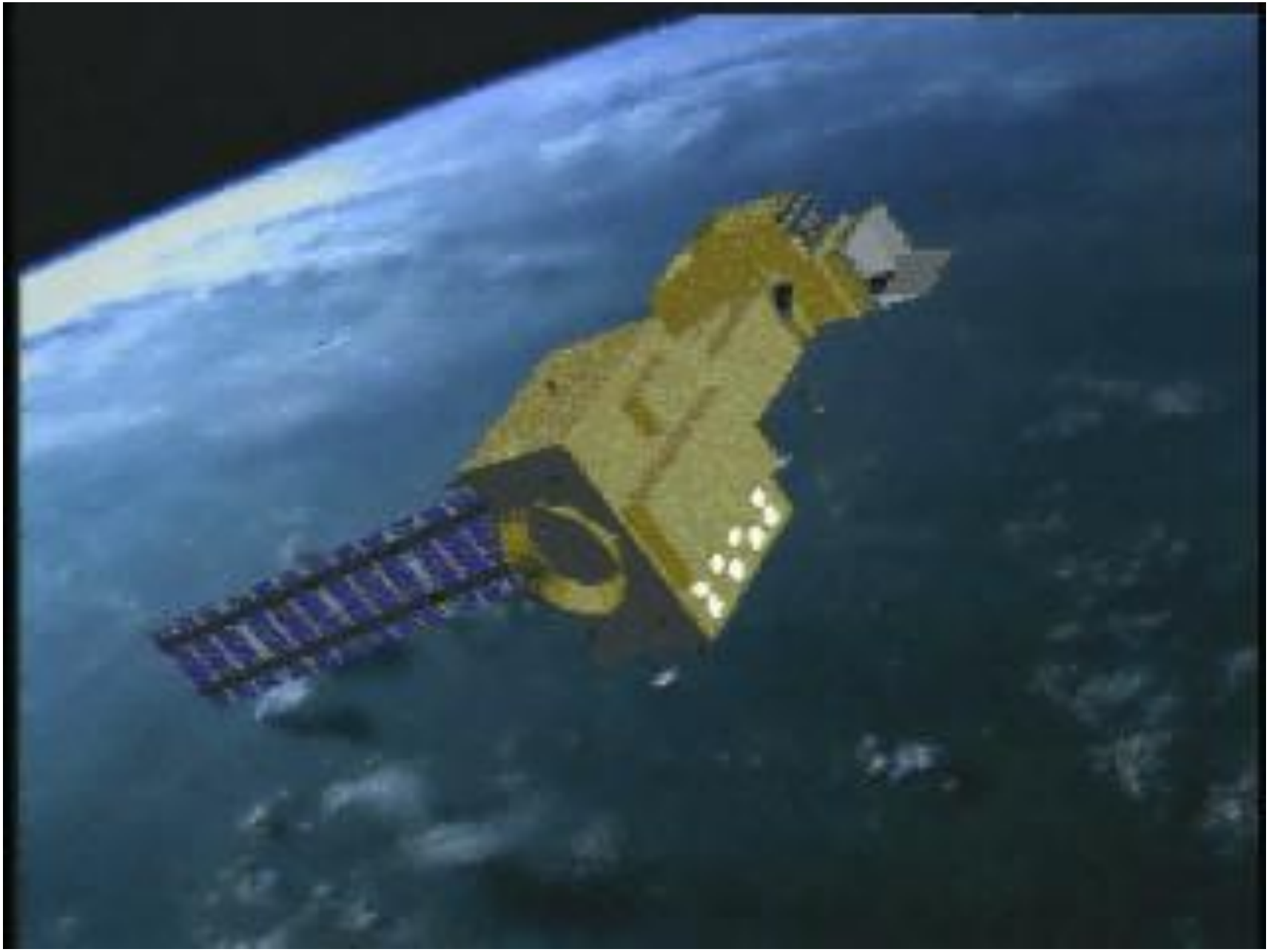

The Plasma Sheet of the Earth

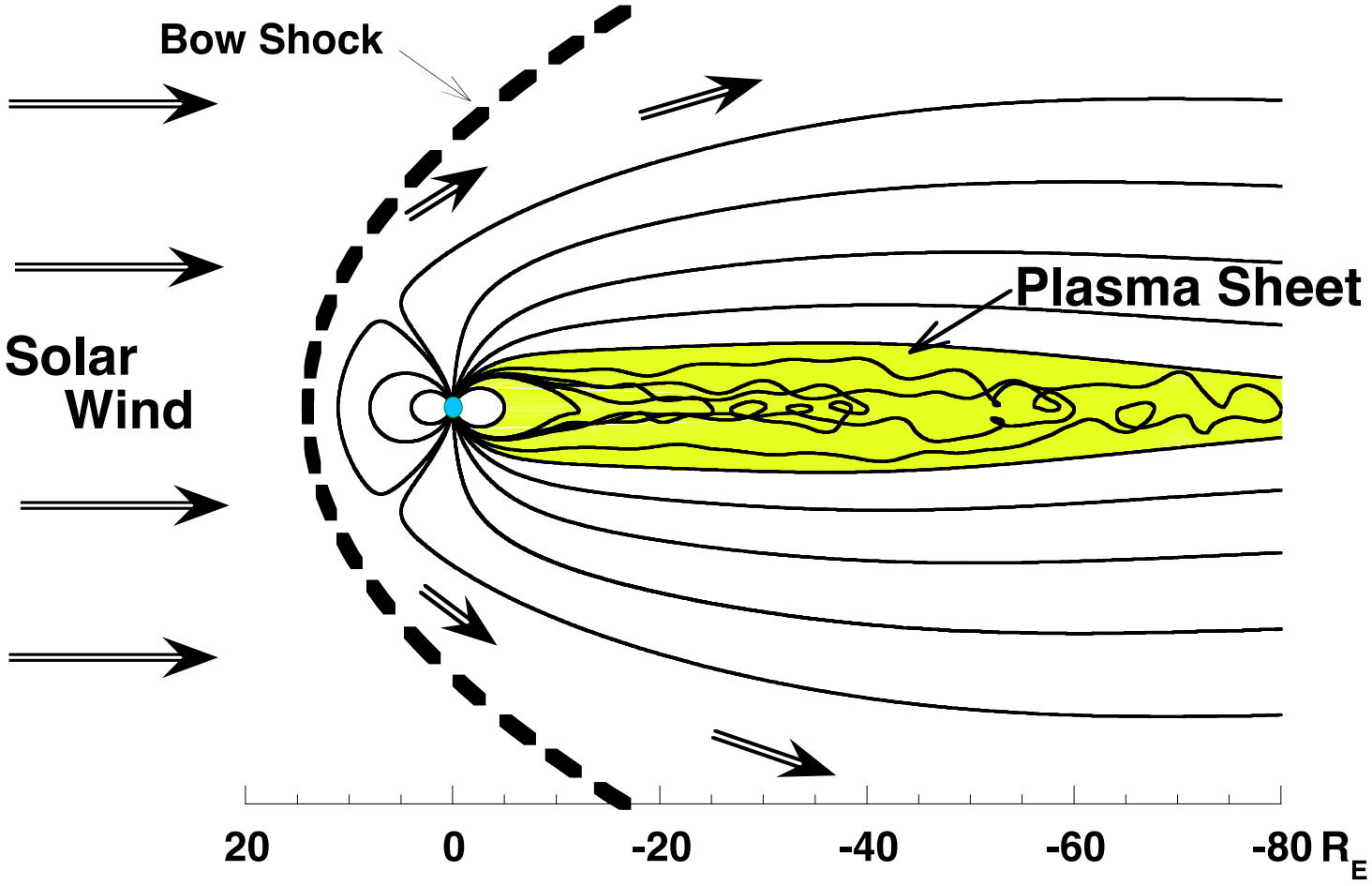

The transport pathways in the plasma sheet are not well understood.

Geosynchronous orbit = 6.6 R_E

Lunar orbit = 60 R_E

Plasma sheet poses spacecraft charging risk to satellites at geosynchronous and low-altitude polar orbits:

- plasma sheet plasma is relatively hot
- the satellites would be be in the dark (Earth's shadow)

Charging Levels in the Plasma Sheet

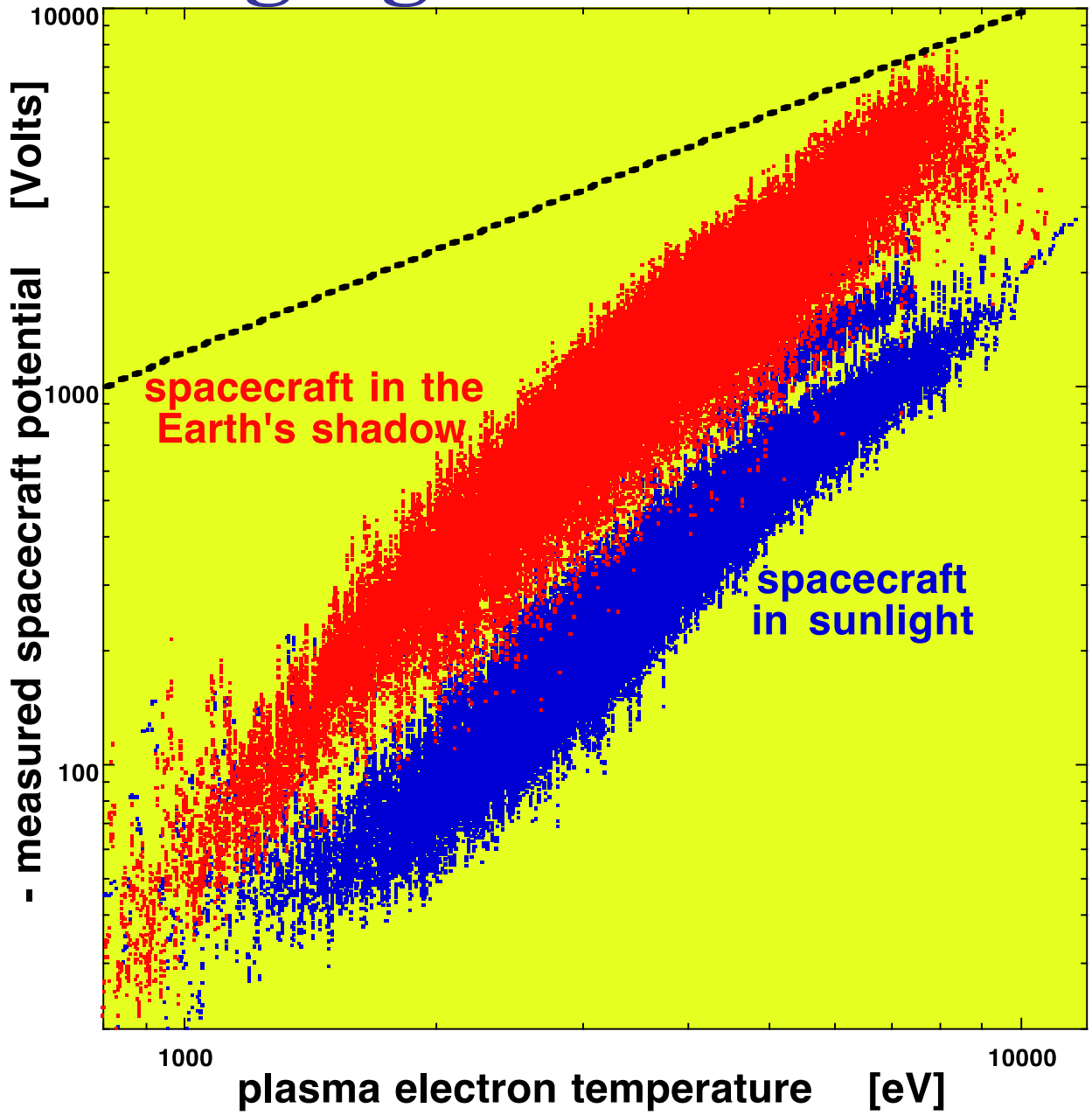

Borovsky [2011]

Remember: darkness is worse than sunlight!

spacecraft charging in the darkness vs. sunlight

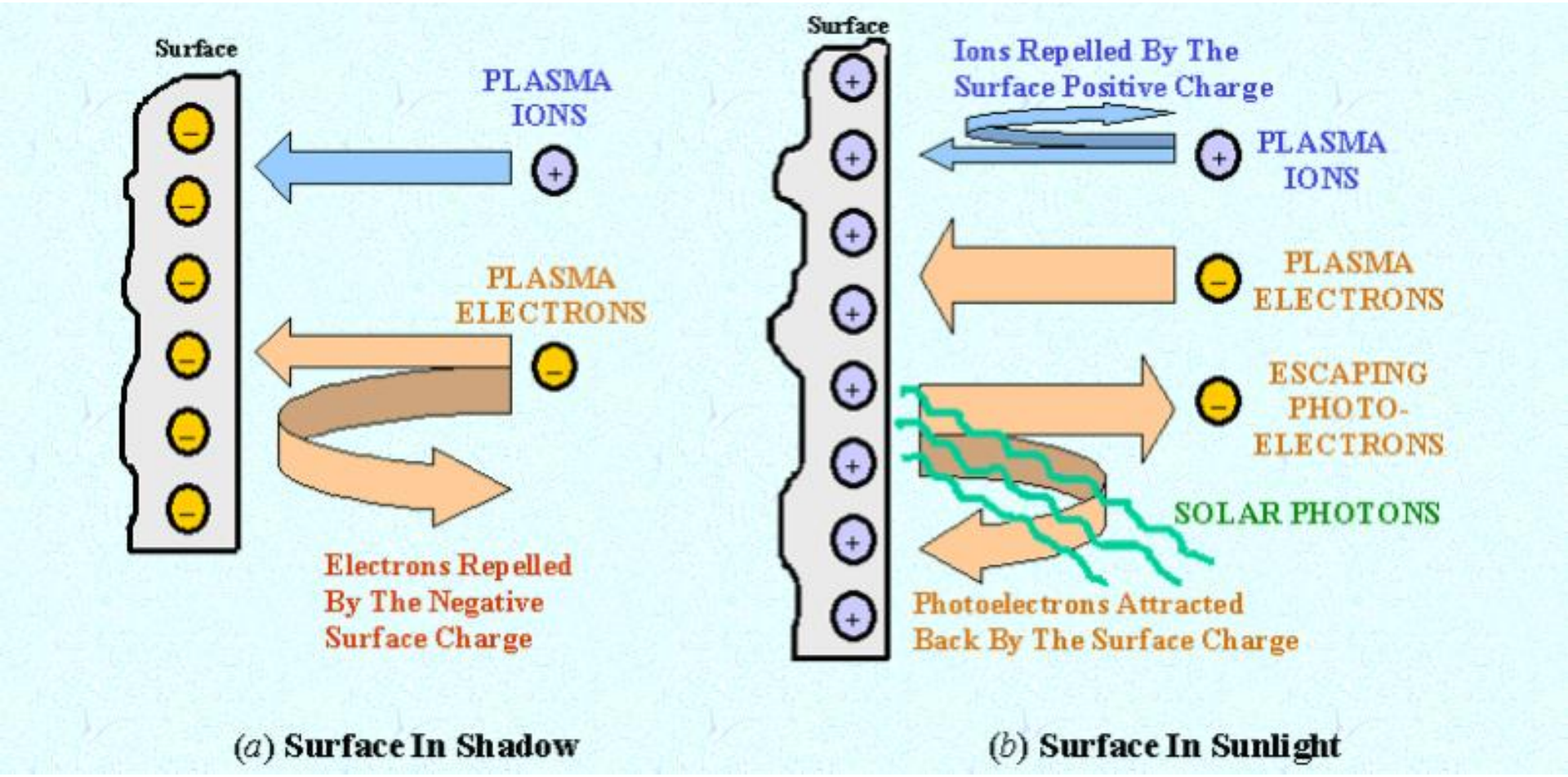

Solar-Cycle Dependence of the Charging Environment

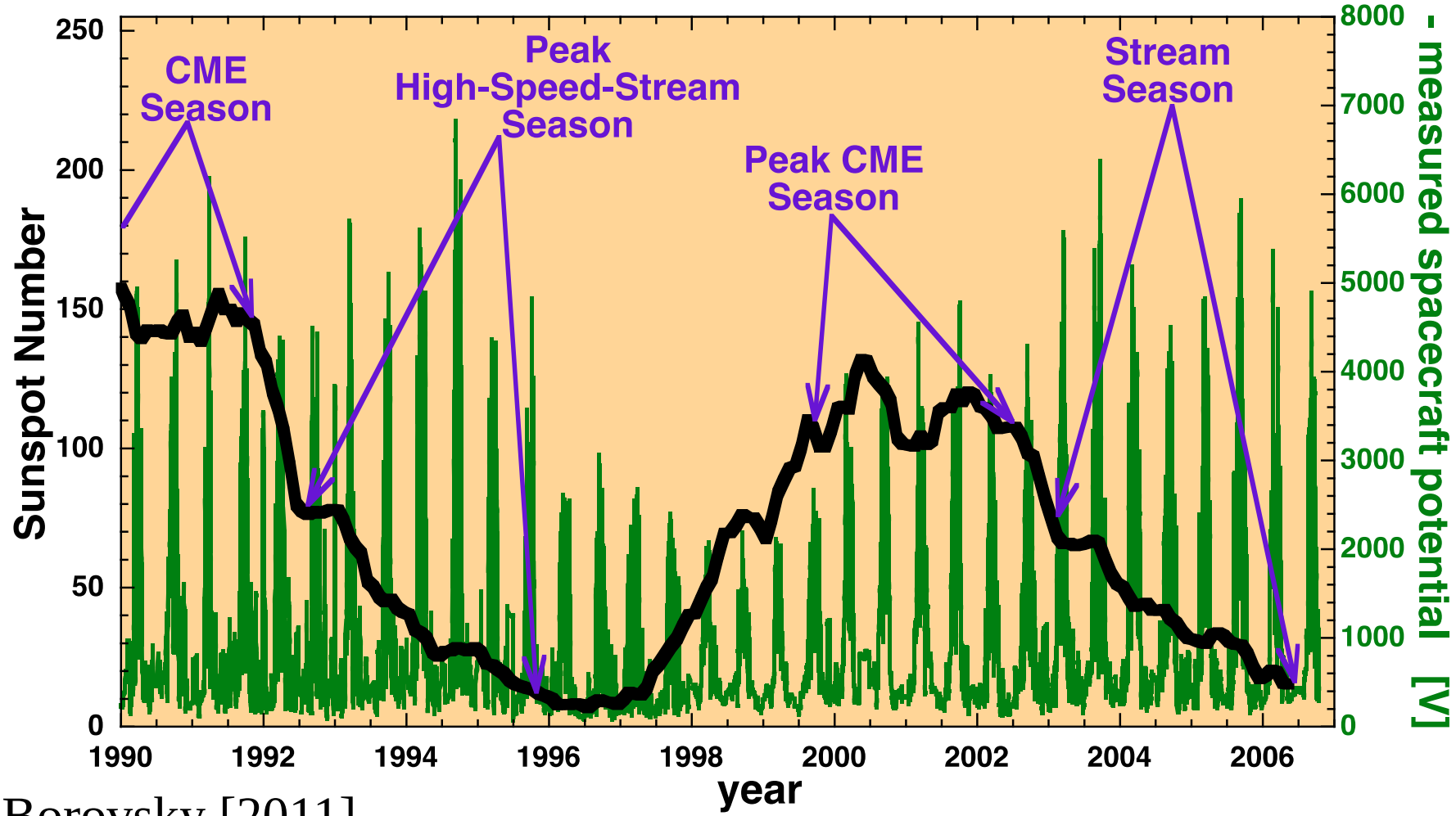

Borovsky [2011]

The high-speed streams of the declining phase bring the most-severe hazards.

energetic electrons and ions can penetrate and damage the instruments on board

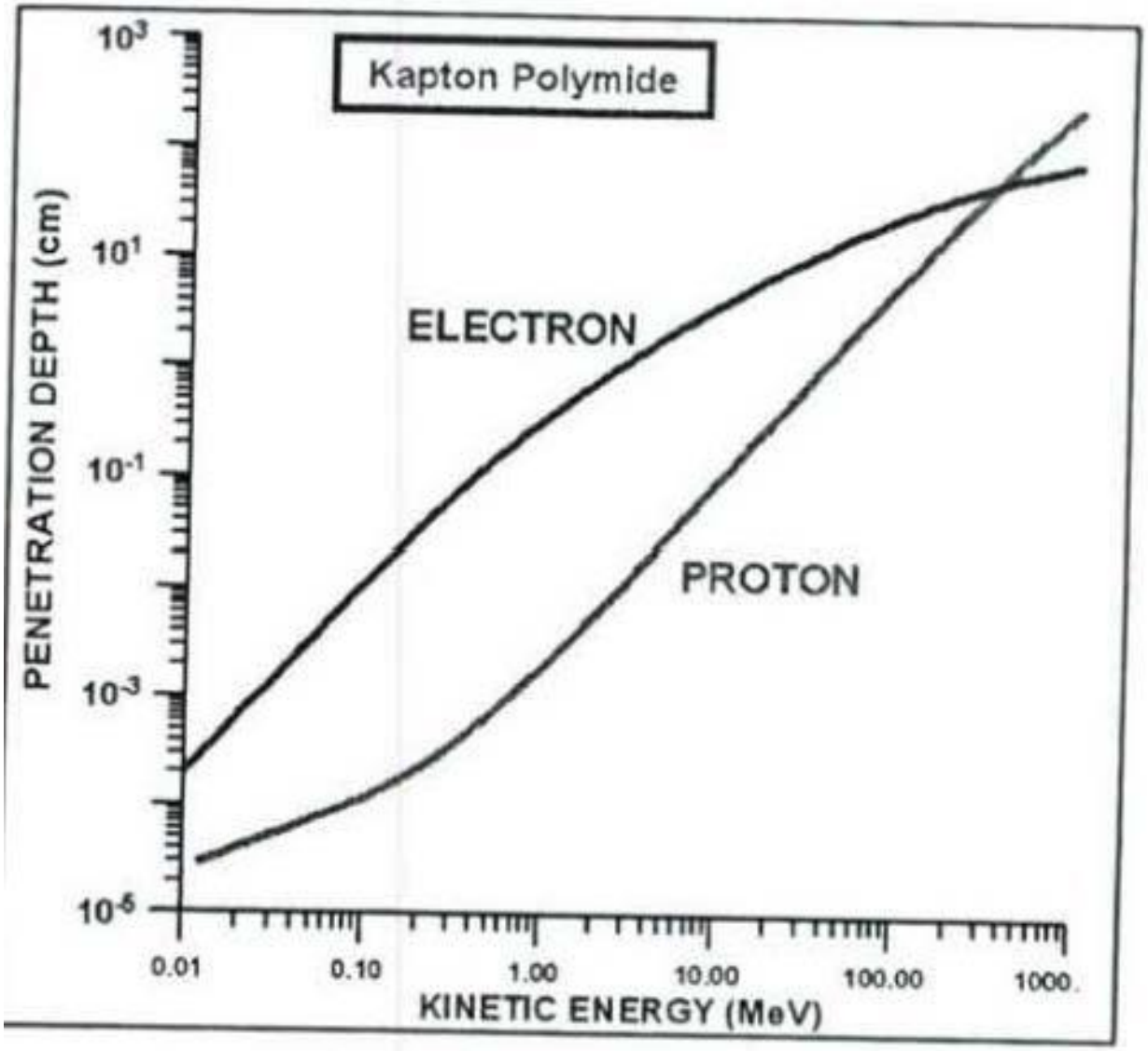

Space weather risks at geosynchronous orbit

Missions Terminated

Due to the Space Environment

Geosynchronous Satellite

VEHICLE	DATE	CAUSE (*)
DSCS II	1973	ESD
GOES 4	1982	ESD
DSP Flight 7	1985	ESD
Feng Yun 1	1988	ESD
MARECS A	1991	ESD
MSTI	1993	SEU
Hipparcos	1993	MRD
Olympus	1993	Meteoroid
SEDS 2	1994	Meteoroid
MSTI 2	1994	Meteoroid
IRON 9906	1997	SEU
INSAT 2D	1997	ESD
TELSTAR401	1998	MRD

(*) ESD = Surface electrostatic discharge
SEU = Single event upset
MRD = MeV radiation dosage

Cause of Failure

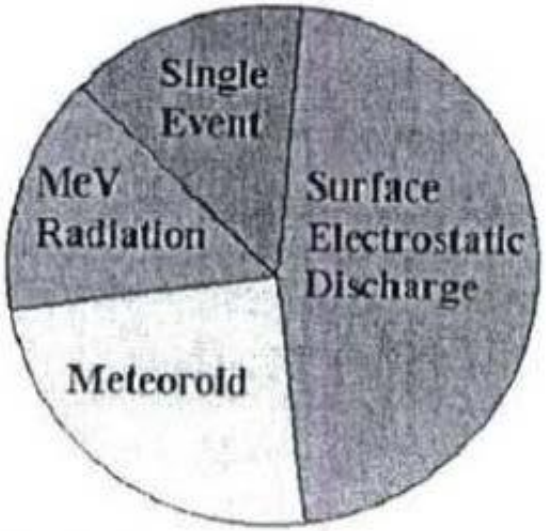

Ref: Koons, et al., SMC-TR-00-10 (2000)

Most Missions Terminated are due to Surface Electrostatic Discharge

- many geosynchronous satellites have terminated/died
- most were due to spacecraft charging

Charging occurs after Te exceed some threshold

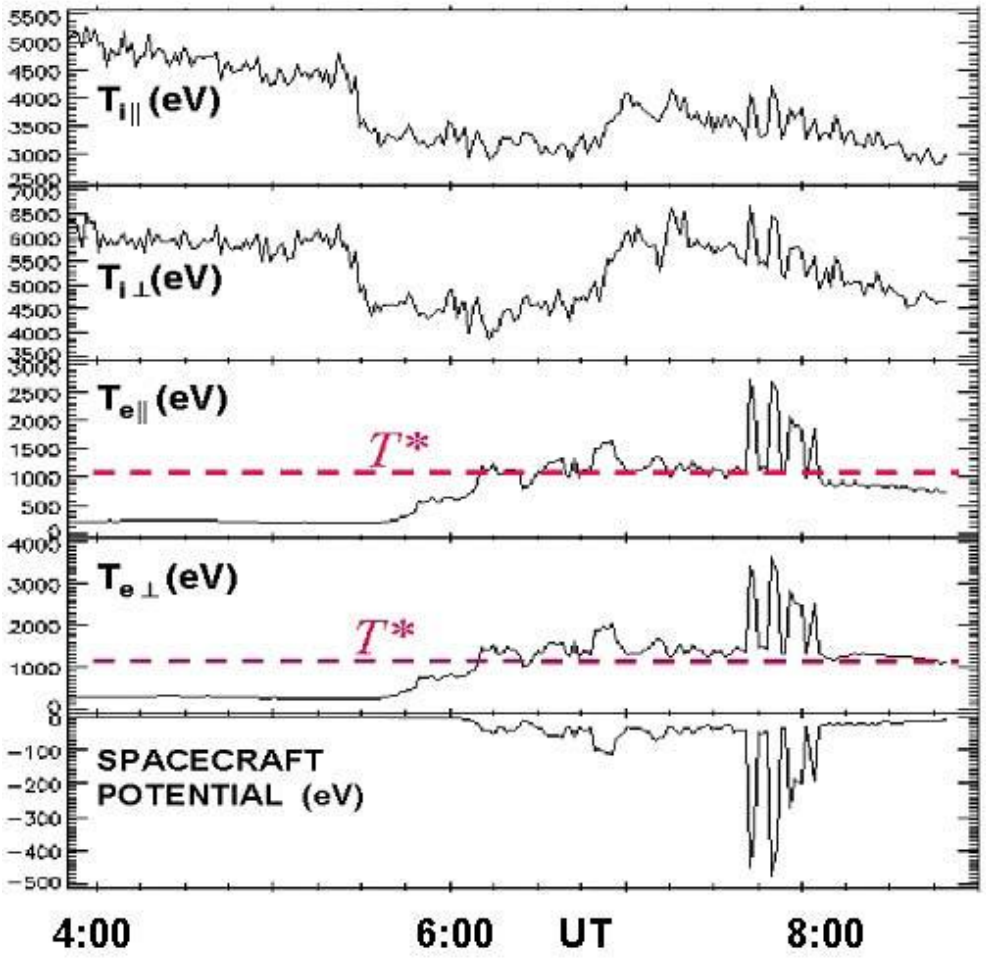

Spacecraft charging on Bastille Day, 2000

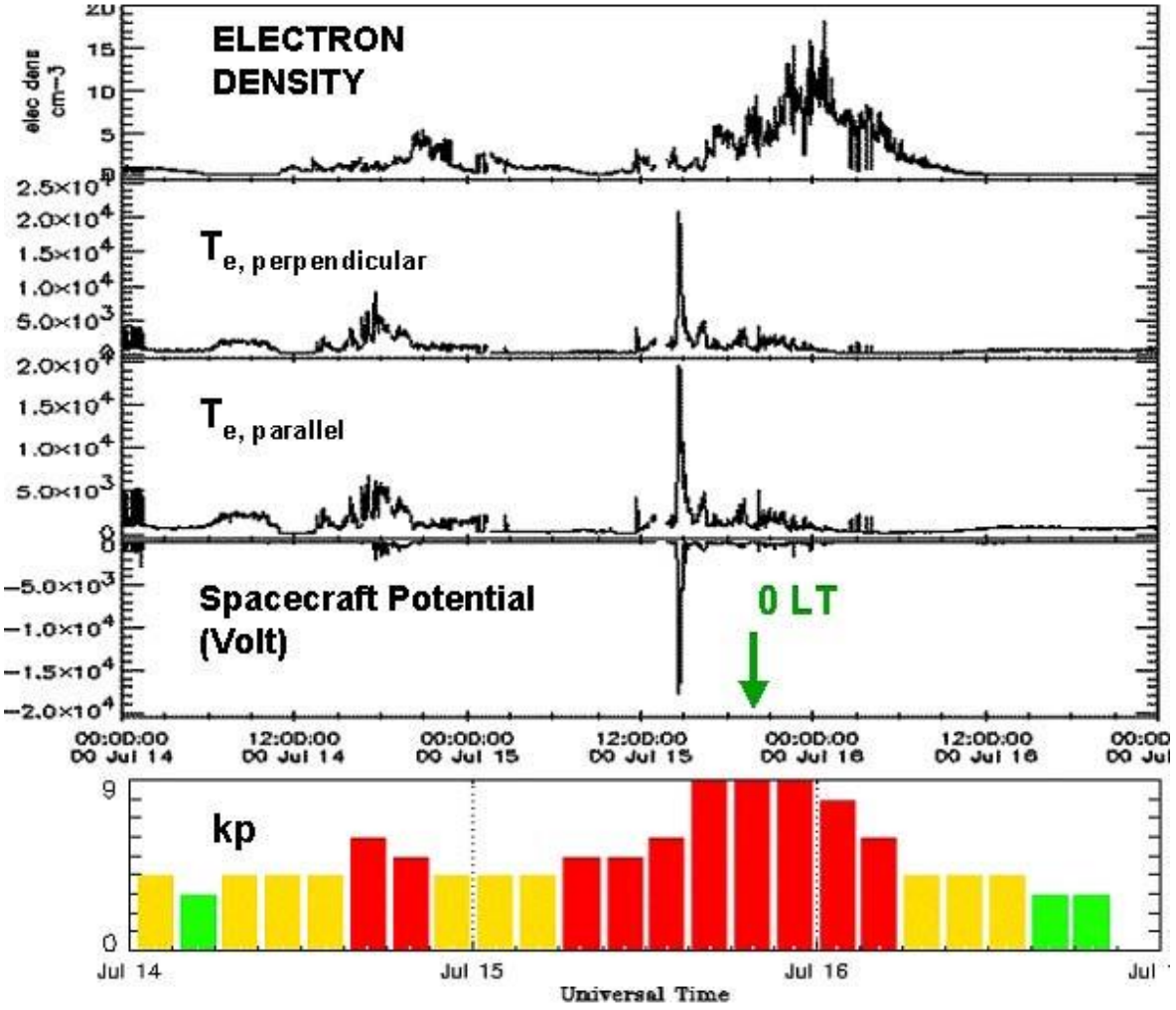

Spacecraft potential is about 3 times larger than that during the peak of HSS season

Lai and Tautz [2006]

3. Researching geosynchronous orbit space environment environment

Researching geosynchronous orbit environment

- Bad news: spacecraft charging risk
- Good news:
  - lots of data at geosychronous orbit
  - researching geosynchronous orbit environment does not have to be expensive
- 3 events:
  - 1997 April 11 13:00 – 17:00 UT
  - 1997 Jul 1 18:00 – 21:00 UT
  - 1996 May 12 21:00 – 24:00 UT
- CDAWEB: http://cdaweb.gsfc.nasa.gov/
- Select: OMNI, GOES, and LANL data

Remember: if you know what you are doing, it is not research!

NASA CDAweb

1. http://cdaweb.gsfc.nasa.gov/istp_public/
2. Select the satellites: OMNI, GOES, LANL

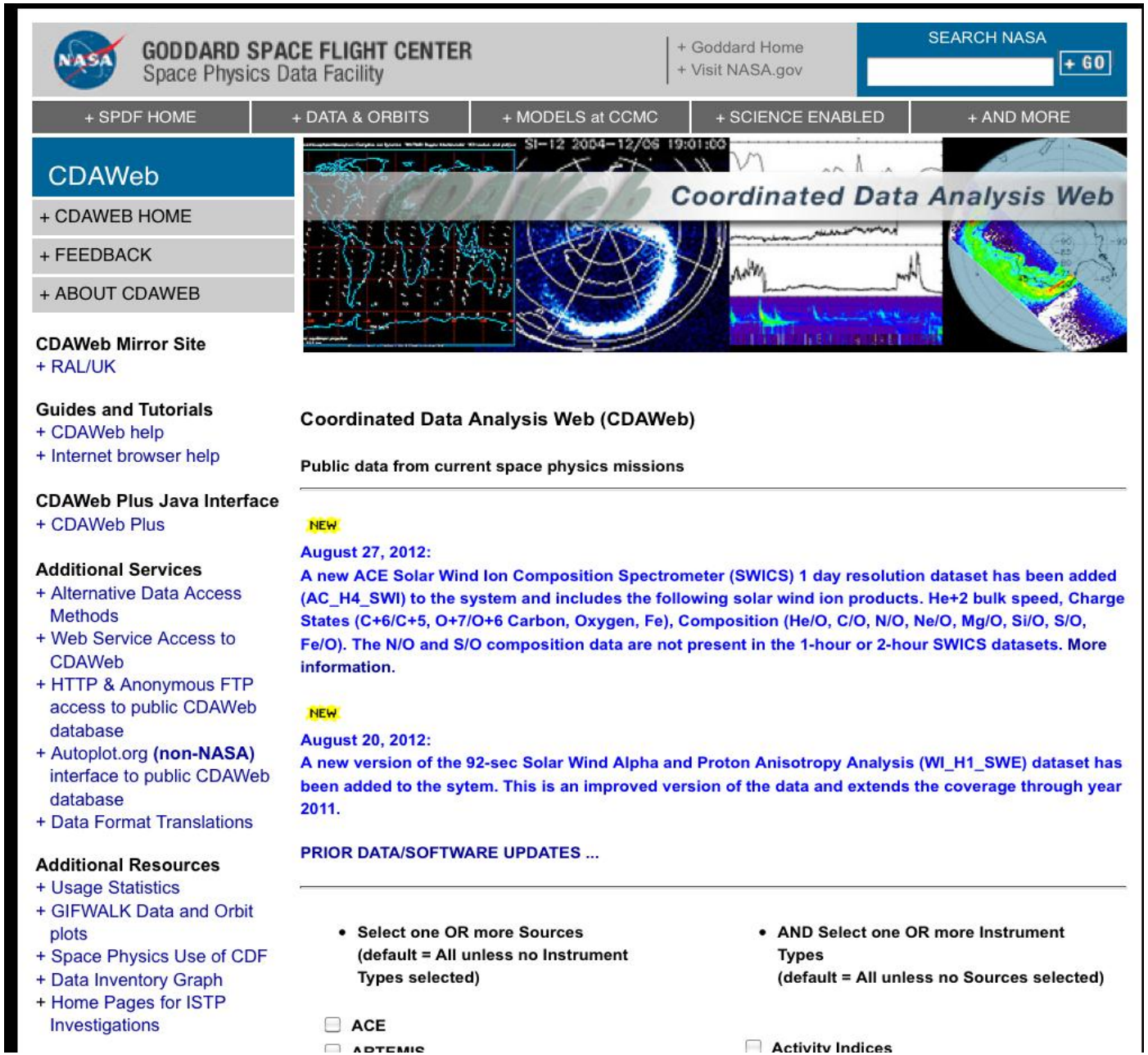

G9_K0_MAG

GOES 9 Magnetometer Key Parameters - H. Singer (NOAA SEC)

Available dates: 1995/12/01 00:00:30 - 1998/07/27 23:59:30
(Continuous coverage not guaranteed - check the inventory graph for coverage)

- [ ] Magnetic Field, GSE
- [x] Magnetic Field (GSM)
- [x] Magnetic Field, local s/c coord
- [x] GOES-9 position, Geographic
- [ ] GOES-9 position, GEO
- [ ] GOES-9 position, GSE
- [ ] GOES-9 position, GSM
- [ ] MGF Instrument Status: 0=OK, 1=minor problems, 2=major problems, 3=missing data

L9_K0_MPA

LANL 1989 Magnetospheric Plasma Analyzer Key Parameters - Mike Henderson (LANL)

Available dates: 1993/03/15 00:05:23 - 2008/01/03 18:20:59
(Continuous coverage not guaranteed - check the inventory graph for coverage)

- [x] Partial density of low energy ions (1-130 eV/e)
- [x] Velocity, 3 comp. in s/c coord., of low energy ions (1-130 eV/e)
- [x] Partial density of high energy ions (.13-45 keV/e)
- [x] Temperatures, parallel & perp. for high energy ions (.13-45 keV/e)
- [ ] Proton symmetry axis: polar ang. relative to Earth direction, azim. ang. from north
- [ ] Ratio Tperp/Tmid for high energy ions, (.13-45 keV/e)
- [x] Partial density of electrons (.03-45 keV/q)
- [x] Temperatures, parallel & perp. for electrons (.03-45 keV/q)
- [ ] Electron symmetry axis: polar ang. relative to Earth direction azim. ang. from north
- [ ] Ratio Tperp/Tmid for electrons (.03-45 keV/q)
- [x] Spacecraft potential
- [ ] Background count rate
- [ ] S/C position, Geographic coordinates (radius,lat,long)
- [x] S/C position, Magnetic coordinates (radius,mlat,mlt)

OMNI_HRO_1MIN

OMNI Combined, Definitive, 1AU 1minute IMF and Plasma data - J.H. King, N. Papatashvilli (AdnetSystems, NASA GSFC)

Available dates: 1995/01/01 00:00:00 - 2012/08/29 23:59:00
(Continuous coverage not guaranteed - check the inventory graph for coverage)

- [ ] OMNI ID code for IMF source spacecraft (see OMNI documentation link for codes)
- [ ] OMNI ID code for IP plasma source spacecraft (see OMNI documentation link for codes)
- [ ] Number of fine time scale points in IMF averages
- [ ] Number of fine time scale points in plasma averages
- [ ] Percent interpolated
- [ ] Timeshift (seconds)
- [ ] RMS Timeshift (seconds)
- [ ] RMS, Phase front normal (nT)
- [ ] Time between observations (seconds)
- [ ] Magnitude of avg. field vector (nT) (last currently-available OMNI B-field data Aug 10, 2012)
- [x] Bx (nT), GSE
- [ ] By (nT), GSE
- [ ] Bz (nT), GSE
- [x] By (nT), GSM, determined from post-shift GSE components
- [x] Bz (nT), GSM, determined from post-shift GSE components
- [ ] RMS SD B scalar (nT)
- [ ] RMS SD field vector (nT)
- [x] Flow Speed (km/s), GSE
- [ ] Vx Velocity (km/s), GSE
- [ ] Vy Velocity (km/s), GSE
- [ ] Vz Velocity (km/s), GSE
- [x] Proton density (n/cc) (last currently-available OMNI plasma data Aug 10, 2012)
- [ ] Temperature (K)
- [ ] Flow pressure (nPa)
- [ ] Electric Field (mV/m)
- [ ] Plasma beta
- [ ] Alfven mach number
- [ ] 1AU IP Magnetosonic mach number
- [ ] X s/c (Re), GSE
- [ ] Y s/c (Re), GSE
- [ ] Z s/c (Re), GSE
- [ ] Bow Shock Nose (Re) location, X, GSE
- [ ] Bow Shock Nose (Re) location, Y, GSE
- [ ] Bow Shock Nose (Re) location, Z, GSE
- [x] AE - 1-minute AE-index, from WDC Kyoto (95/001-12/213)
- [x] AL - 1-minute AL-index, from WDC Kyoto (95/001-12/213)
- [ ] AU - 1-minute AU-index,from WDC Kyoto (95/001-12/213)
- [ ] SYM/D - 1-minute SYM/D index,from WDC Kyoto (95/001-12/213)
- [x] SYM/H - 1-minute SYM/H index,from WDC Kyoto (95/001-12/213)
- [ ] ASY/D - 1-minute ASY/D index,from WDC Kyoto (95/001-12/213)
- [ ] ASY/H - 1-minute ASY/H index,from WDC Kyoto (95/001-12/213)

- [ ] G6_K0_EPS: GOES 6 Energetic Particle Sensor, Key Parameters - H. Sauer (NOAA)
  [Available Time Range: 1992/12/12 00:02:30 - 1994/11/25 23:57:30]
- [ ] G6_K0_MAG: GOES-6 Magnetometer Key Parameters - R. Zwickl (NOAA SEL)
  [Available Time Range: 1992/12/12 00:00:30 - 1994/11/25 23:59:30]
- [ ] G7_K0_EPS: GOES 7 Energetic Particle Sensor, Key Parameters - H. Sauer (NOAA)
  [Available Time Range: 1992/12/12 00:02:30 - 1996/02/26 23:57:30]
- [ ] G7_K0_MAG: GOES-7 Magnetometer Key Parameters - R. Zwickl (NOAA SEL)
  [Available Time Range: 1992/12/12 00:00:30 - 1996/02/26 23:59:30]
- [ ] G7_K1_MAG: GOES-7 Magnetometer Calculated PSD for Hn - R. Zwickl (NOAA SEL)
  [Available Time Range: 1995/02/11 04:00:30 - 1995/04/09 00:59:30]
- [ ] G8_K0_EPS: GOES 8 Energetic Particle Sensor, Key Parameters - T. Onsager (NOAA SEC)
  [Available Time Range: 1995/12/01 00:02:30 - 2003/04/08 23:57:30]
- [x] G8_K0_MAG: GOES 8 Magnetometer Key Parameters - H. Singer (NOAA SEC)
  [Available Time Range: 1995/12/01 00:00:30 - 2003/04/08 23:59:30]
- [ ] G9_K0_EPS: GOES 9 Energetic Particle Sensor, Key Parameters - T. Onsager (NOAA SEC)
  [Available Time Range: 1995/12/01 00:02:30 - 1998/07/27 23:57:30]
- [x] G9_K0_MAG: GOES 9 Magnetometer Key Parameters - H. Singer (NOAA SEC)
  [Available Time Range: 1995/12/01 00:00:30 - 1998/07/27 23:59:30]
- [ ] G0_K0_EPS: GOES 10 Energetic Particle Sensor, Key Parameters - T. Onsager (NOAA SEC)
  [Available Time Range: 1999/03/21 00:02:30 - 2006/06/22 23:57:30]
- [ ] G0_K0_MAG: GOES 10 Magnetometer Key Parameters - H. Singer (NOAA SEC)
  [Available Time Range: 1999/03/21 00:00:30 - 2006/06/22 23:59:30]
- [ ] G10_L2_MAG: GOES-10 High Resolution Magnetometer data vectors (at 512 ms, ephem at 60 sec) - Howard J. Singer (NOAA Space Weather Prediction Center)
  [Available Time Range: 2007/01/01 00:00:00 - 2008/12/31 23:59:59]
- [ ] GOES11_K0_EPS: GOES 11 Energetic Particle Sensor, Key Parameters - T. Onsager (NOAA SEC)
  [Available Time Range: 2006/06/23 00:02:30 - 2010/12/30 23:57:30]
- [ ] GOES11_K0_MAG: GOES 11 Magnetometer Key Parameters - H. Singer (NOAA SEC)
  [Available Time Range: 2006/06/23 00:00:30 - 2010/12/30 23:59:30]
- [ ] G11_L2_MAG: GOES-11 High Resolution Magnetometer data vectors (at 512 ms, ephem at 60 sec) - Howard J. Singer (NOAA Space Weather Prediction Center)
  [Available Time Range: 2007/01/01 00:00:00 - 2008/12/31 23:59:59]
- [ ] GOES12_K0_EPS: GOES 12 Energetic Particle Sensor, Key Parameters - T. Onsager (NOAA SEC)
  [Available Time Range: Select dataset for details]
- [ ] GOES12_K0_MAG: GOES 12 Magnetometer Key Parameters - H. Singer (NOAA SEC)
  [Available Time Range: 2003/04/08 00:00:30 - 2010/09/23 23:59:30]
- [ ] G12_L2_MAG: GOES-12 High Resolution Magnetometer data vectors (at 512 ms, ephem at 60 sec) - Howard J. Singer (NOAA Space Weather Prediction Center)
  [Available Time Range: 2007/01/01 00:00:00 - 2008/12/31 23:59:59]
- [ ] A1_K0_MPA: LANL 2001 Magnetospheric Plasma Analyzer Key Parameters - Mike Henderson (LANL)
  [Available Time Range: Select dataset for details]
- [ ] A2_K0_MPA: LANL 2002 Magnetospheric Plasma Analyzer Key Parameters - Mike Henderson (LANL)
  [Available Time Range: Select dataset for details]
- [ ] L9_H0_MPA: LANL 1989-046 Magnetospheric Plasma Analyzer High Resolution data - Mike Henderson (LANL)
  [Available Time Range: 1998/05/03 04:12:36 - 1998/05/03 07:42:38]
- [x] L9_K0_MPA: LANL 1989 Magnetospheric Plasma Analyzer Key Parameters - Mike Henderson (LANL)
  [Available Time Range: 1993/03/15 00:05:23 - 2008/01/03 18:20:59]
- [x] L9_K0_SPA: LANL 1989 Synchronous Orbit Particle Analyzer Key Parameters - Reiner Friedel (LANL)
  [Available Time Range: 1992/08/01 00:00:27 - 2007/10/15 23:58:30]
- [x] L0_K0_MPA: LANL 1990 Magnetospheric Plasma Analyzer Key Parameters - Mike Henderson (LANL)
  [Available Time Range: 1992/12/16 00:02:44 - 2005/11/09 23:57:44]
- [x] L0_K0_SPA: LANL 1990 Synchronous Orbit Particle Analyzer Key Parameters - Reiner Friedel (LANL)
  [Available Time Range: 1992/08/01 00:00:32 - 2005/11/09 23:58:30]
- [x] L1_K0_MPA: LANL 1991 Magnetospheric Plasma Analyzer Key Parameters - Mike Henderson (LANL)
  [Available Time Range: 1993/10/27 01:31:20 - 2004/11/23 18:14:22]
- [x] L1_K0_SPA: LANL 1991 Synchronous Orbit Particle Analyzer Key Parameters - Reiner Friedel (LANL)
  [Available Time Range: 1992/08/01 00:00:26 - 2004/11/23 18:16:33]
- [x] L4_K0_MPA: LANL 1994 Magnetospheric Plasma Analyzer Key Parameters - Mike Henderson (LANL)
  [Available Time Range: 1996/01/01 00:01:40 - 2008/01/03 02:25:58]
- [ ] L4_K0_SPA: LANL 1994 Synchronous Orbit Particle Analyzer Key Parameters - Reiner Friedel (LANL)
  [Available Time Range: 1996/02/16 00:00:37 - 2007/10/15 23:58:31]
- [ ] L7_H0_MPA: LANL 1997 Magnetospheric Plasma Analyzer High Resolution data - Mike Henderson (LANL)
  [Available Time Range: 1998/04/29 00:02:23 - 1998/05/09 23:57:09]
- [ ] L7_K0_MPA: LANL 1997 Magnetospheric Plasma Analyzer Key Parameters - Mike Henderson (LANL)
  [Available Time Range: 1997/07/04 23:00:13 - 2008/01/03 18:21:15]
- [ ] L7_K0_SPA: LANL 1997 Synchronous Orbit Particle Analyzer Key Parameters - Reiner Friedel (LANL)
  [Available Time Range: 1999/01/01 00:00:31 - 2007/10/15 23:58:28]
- [x] OMNI_HRO_1MIN: OMNI Combined, Definitive, 1AU 1minute IMF and Plasma data - J.H. King, N. Papatashvilli (AdnetSystems, NASA GSFC)
  [Available Time Range: 1995/01/01 00:00:00 - 2012/08/29 23:59:00]
- [ ] OMNI_HRO_5MIN: OMNI Combined, Definitive, 1AU 5minute IMF and Plasma data - J.H. King, N. Papatashvilli (AdnetSystems, NASA GSFC)
  [Available Time Range: 1995/01/01 00:00:00 - 2012/08/29 23:55:00]
- [ ] OMNI2_H0_MRG1HR: OMNI Combined, Definitive, 1AU Hourly IMF, Plasma, Energetic Proton Fluxes, and Solar and Magnetic Indices - J.H. King, N. Papatashvilli (ADNET, NASA GSFC)
  [Available Time Range: 1963/01/01 00:00:00 - 2012/08/31 16:00:00]
- [ ] OMNI_COHO1HR_MERGED_MAG_PLASMA: OMNI Combined merged hourly magnetic field, plasma and ephermis data - J.H. King, N. Papatashvilli (AdnetSystems, NASA GSFC)
  [Available Time Range: 1963/01/01 00:00:00 - 2012/08/29 00:00:00]
- [ ] L1_K0_GIFWALK: Links to GEOSYNC KP pre-generated survey and other plots - Polar-Wind-Geotail Ground System (NASA GSFC)
  [Available Time Range: Select dataset for details]
- [ ] G0_K0_GIFWALK: Links to GEOSYNC KP pre-generated survey and other plots - Polar-Wind-Geotail Ground System (NASA GSFC)
  [Available Time Range: Select dataset for details]

Submit Reset

select:
G8_K0_MAG,
G9_K0_MAG,
L9_K0_MPA,
L0_K0_MPA,
L4_K0_MPA,
L1_K0_MPA,
OMNI_HR0_1
MIN

GSM coordinate system

GEOCENTRIC SOLAR MAGNETOSPHERIC SYSTEM (GSM)

- The geocentric solar magnetospheric system (GSM), as with both the GSE and GSEQ systems, has its *X*-axis from the Earth to the Sun.
- The *Y*-axis is defined to be perpendicular to the Earth's magnetic dipole so that the *X*-*Z* plane contains the dipole axis (positive is duskward).
- The positive *Z*- axis is chosen to be in the same sense as the northern magnetic pole.

1997 April 11 13:00 – 17:00 UT

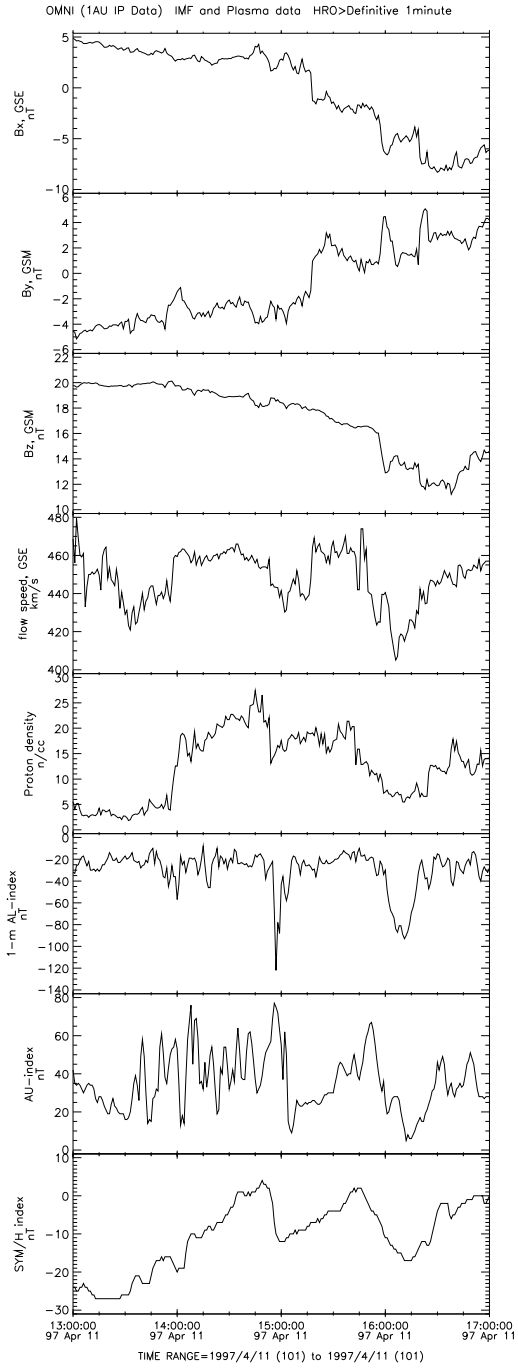

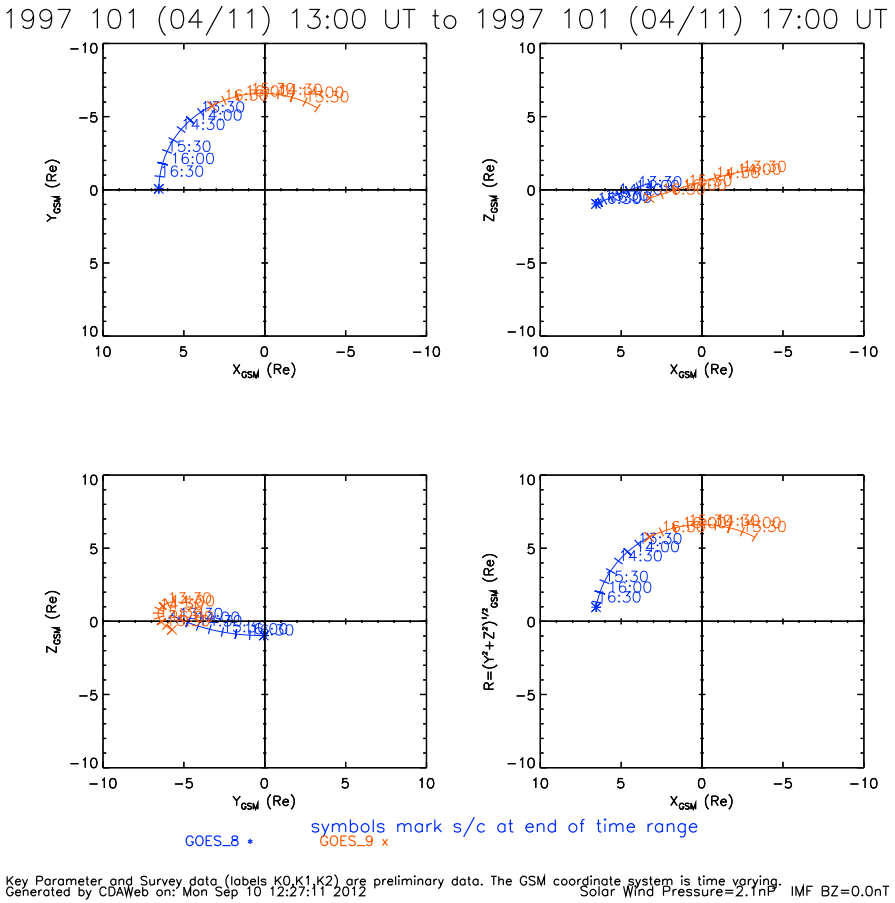

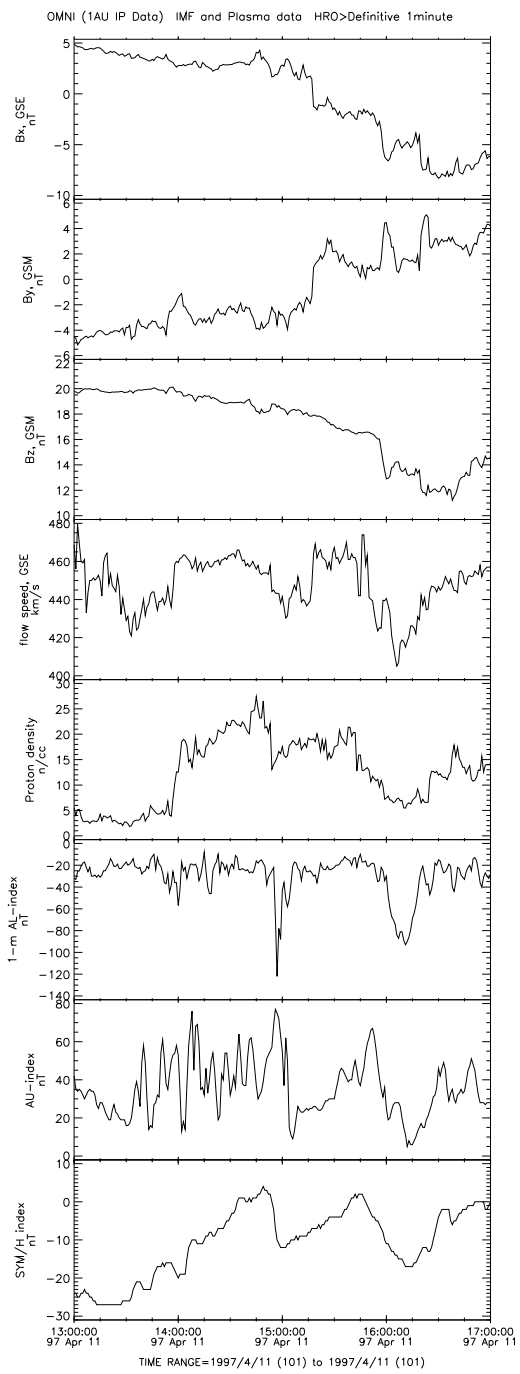
OMNI (1AU IP Data) IMF and Plasma data HRO>Definitive 1minute
Bx, GSE nT
By, GSM nT
Bz, GSM nT
flow speed, GSE km/s
Proton density n/cc
1-m AL-index nT
AU-index nT
SYM/H index nT
13:00:00 97 Apr 11
14:00:00 97 Apr 11
15:00:00 97 Apr 11
16:00:00 97 Apr 11
17:00:00 97 Apr 11
TIME RANGE=1997/4/11 (101) to 1997/4/11 (101)

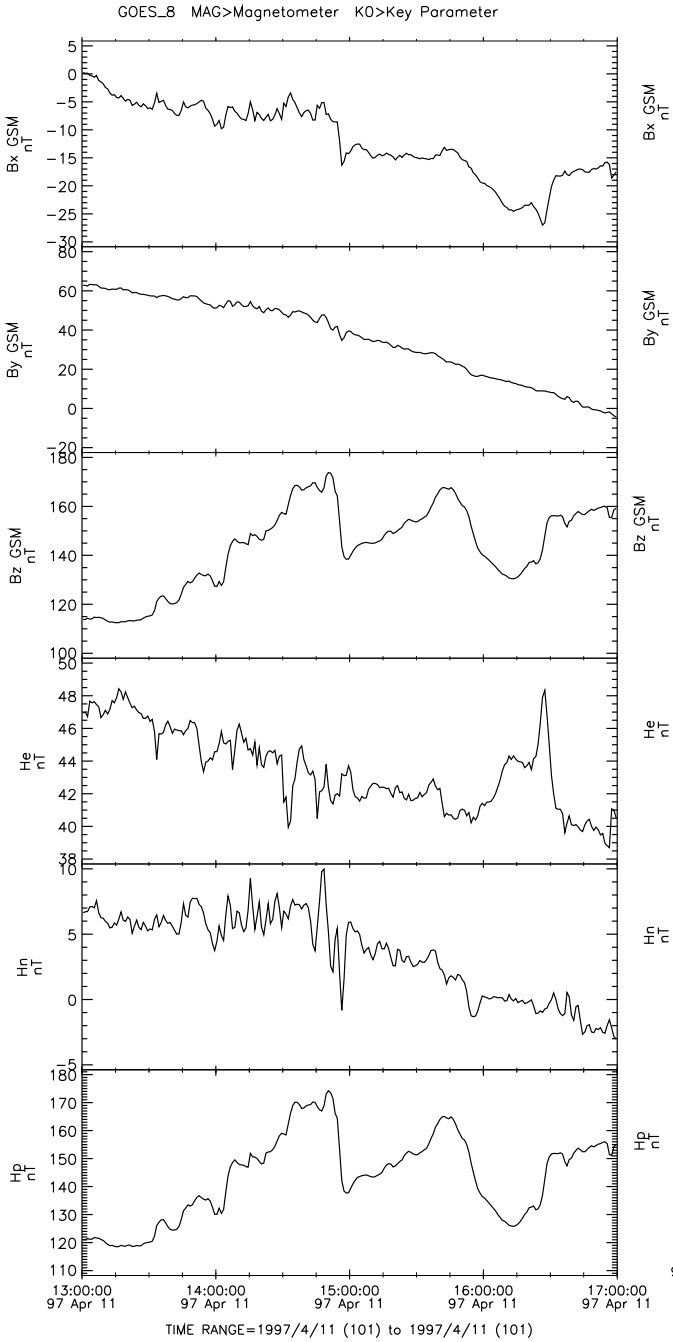
GOES_8 MAG>Magnetometer K0>Key Parameter
Bx GSM nT
By GSM nT
Bz GSM nT
He nT
Hn nT
Hp nT
13:00:00 97 Apr 11
14:00:00 97 Apr 11
15:00:00 97 Apr 11
16:00:00 97 Apr 11
17:00:00 97 Apr 11
TIME RANGE=1997/4/11 (101) to 1997/4/11 (101)

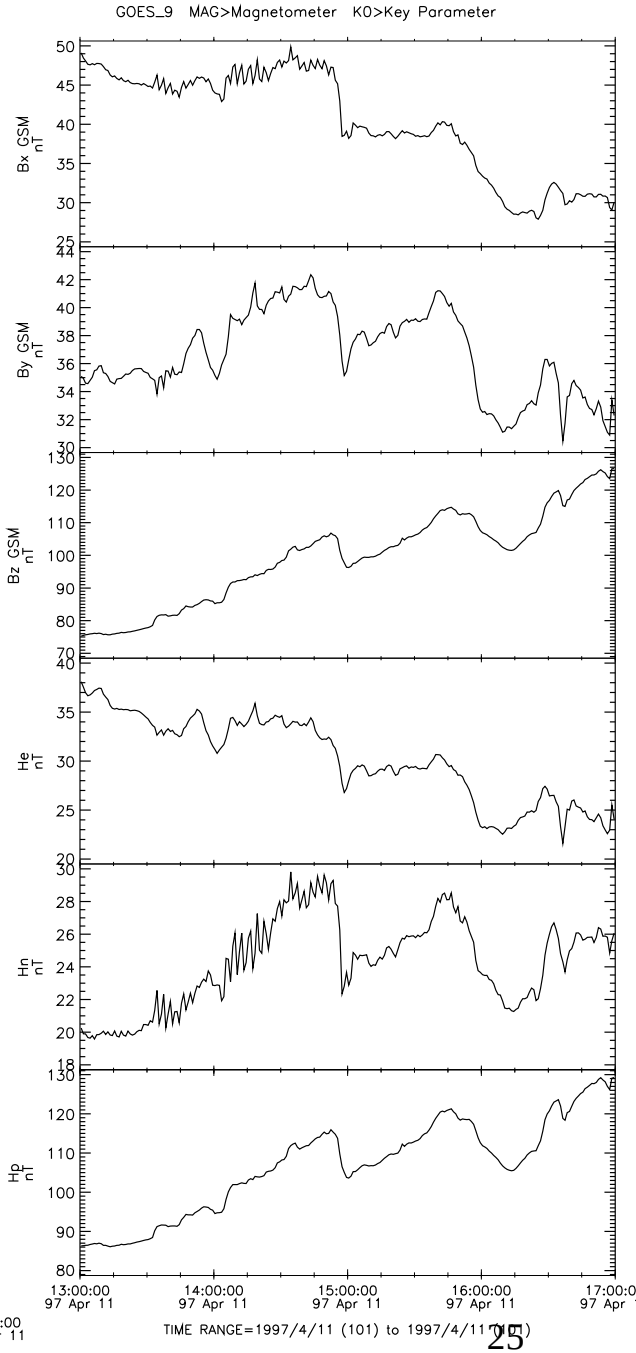
GOES_9 MAG>Magnetometer K0>Key Parameter
Bx GSM nT
By GSM nT
Bz GSM nT
He nT
Hn nT
Hp nT
13:00:00 97 Apr 11
14:00:00 97 Apr 11
15:00:00 97 Apr 11
16:00:00 97 Apr 11
17:00:00 97 Apr 11
TIME RANGE=1997/4/11 (101) to 1997/4/11 (101)

Magnetosphere

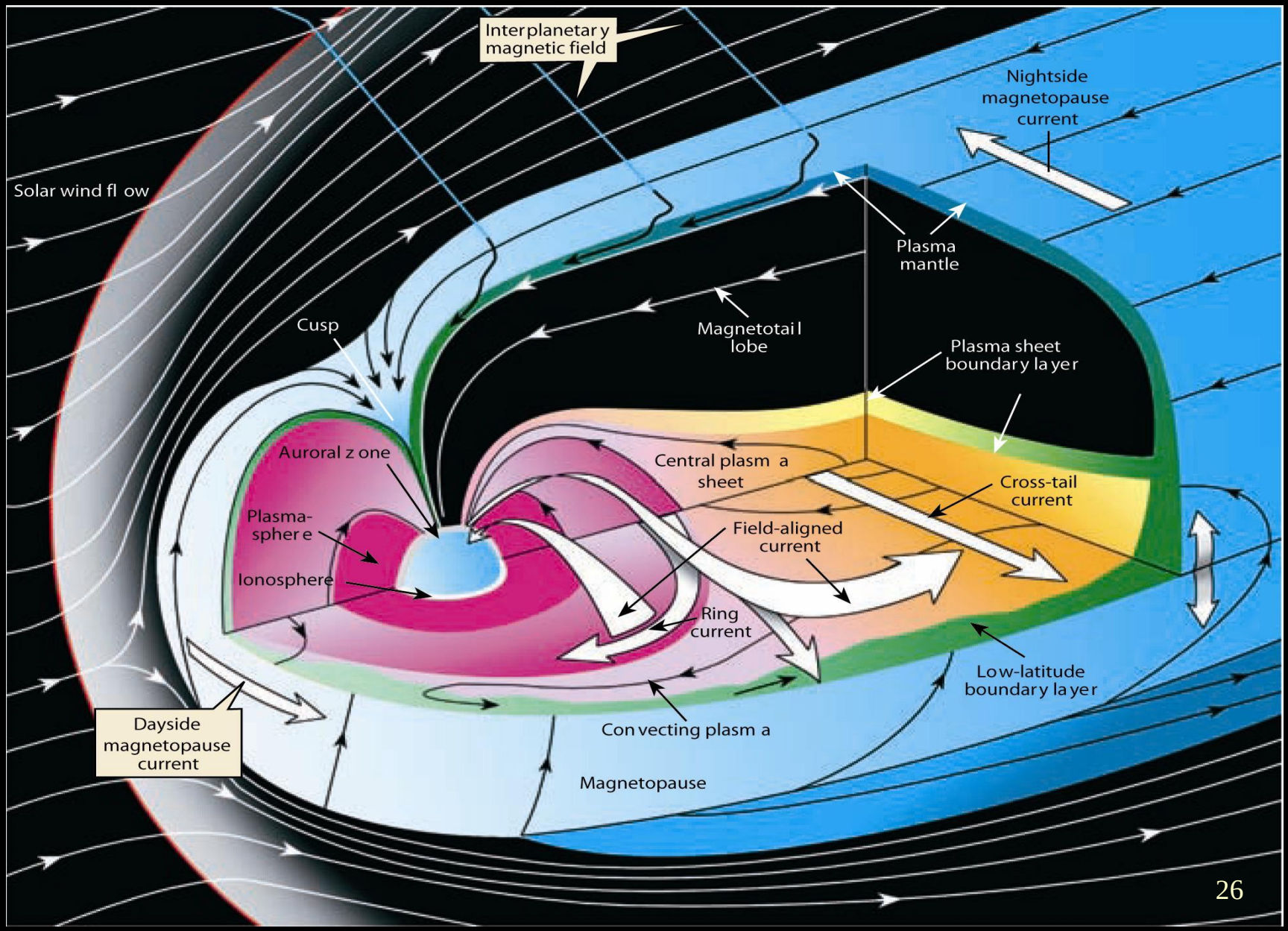

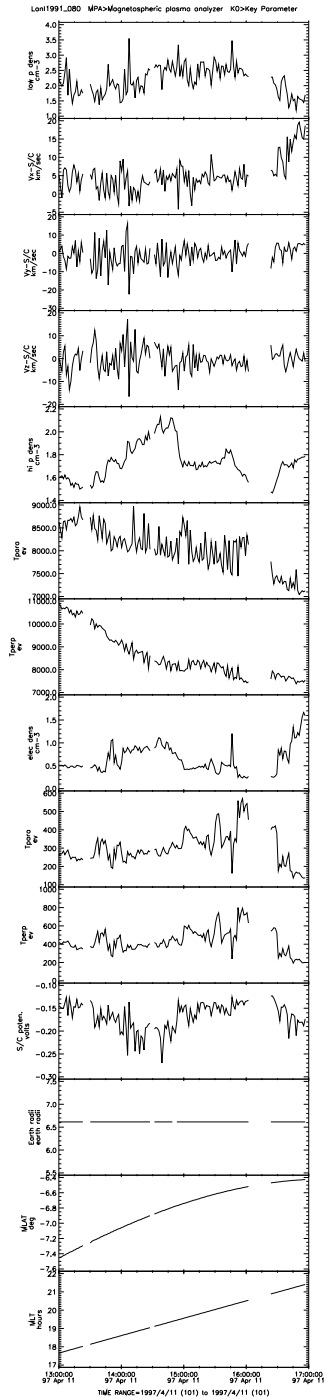
Lanl1991_080 MPA>Magnetospheric plasma analyzer KO>Key Parameter
low p dens cm-3
Vx-S/C km/sec
Vy-S/C km/sec
Vz-S/C km/sec
hi p dens cm-3
Tpara ev
Tperp ev
elec dens cm-3
Tpara ev
Tperp ev
S/C poten. volts
Earth radii earth radii
MLAT deg
MLT hours
13:00:00 97 Apr 11
14:00:00 97 Apr 11
15:00:00 97 Apr 11
16:00:00 97 Apr 11
17:00:00 97 Apr 11
TIME RANGE=1997/4/11 (101) to 1997/4/11 (101)

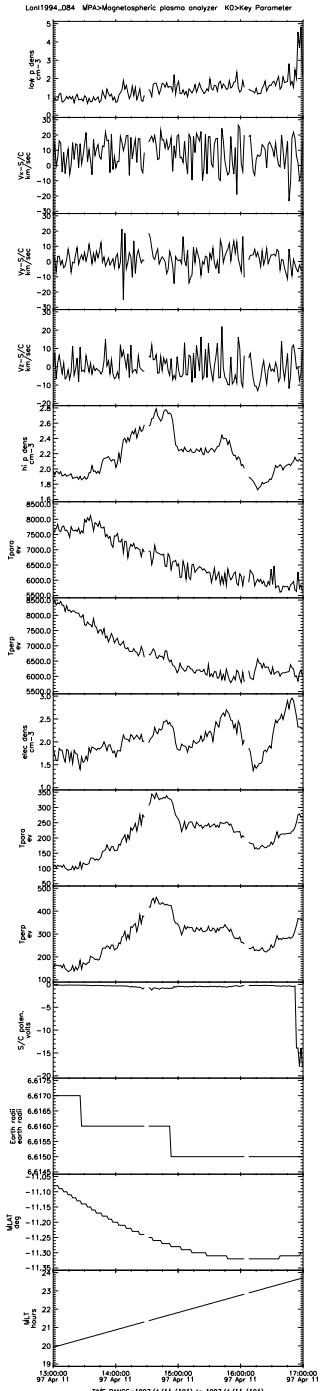
Lanl1994_084 MPA>Magnetospheric plasma analyzer KO>Key Parameter
low p dens cm-3
Vx-S/C km/sec
Vy-S/C km/sec
Vz-S/C km/sec
hi p dens cm-3
Tpara ev
Tperp ev
elec dens cm-3
Tpara ev
Tperp ev
S/C poten. volts
Earth radii earth radii
MLAT deg
MLT hours
13:00:00 97 Apr 11
14:00:00 97 Apr 11
15:00:00 97 Apr 11
16:00:00 97 Apr 11
17:00:00 97 Apr 11

1997 Jul 1 18:00 – 21:00 UT

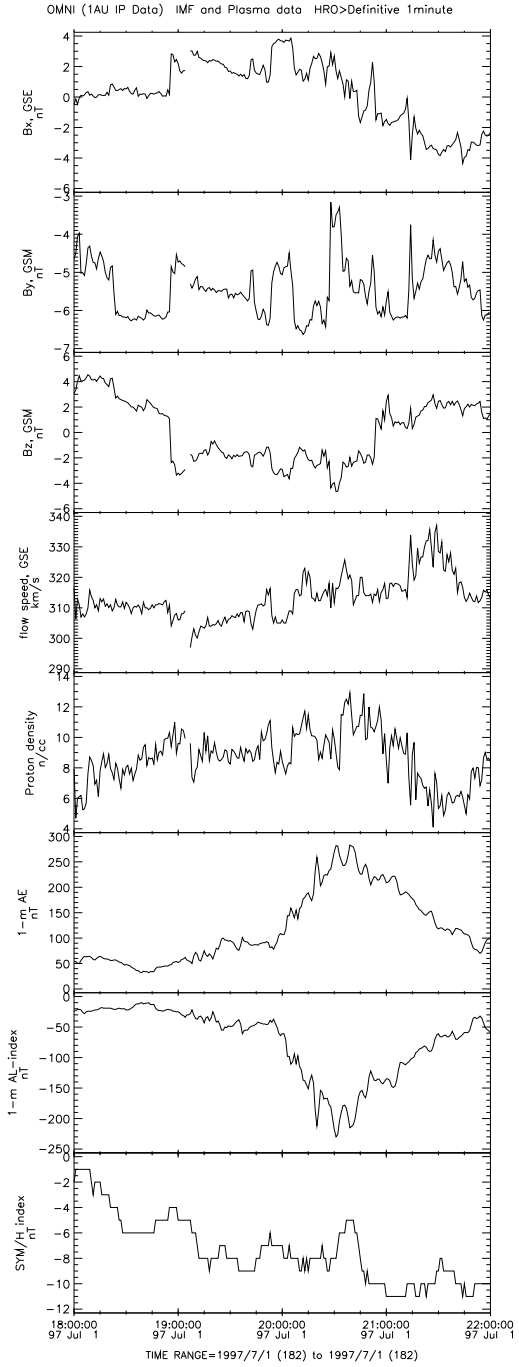

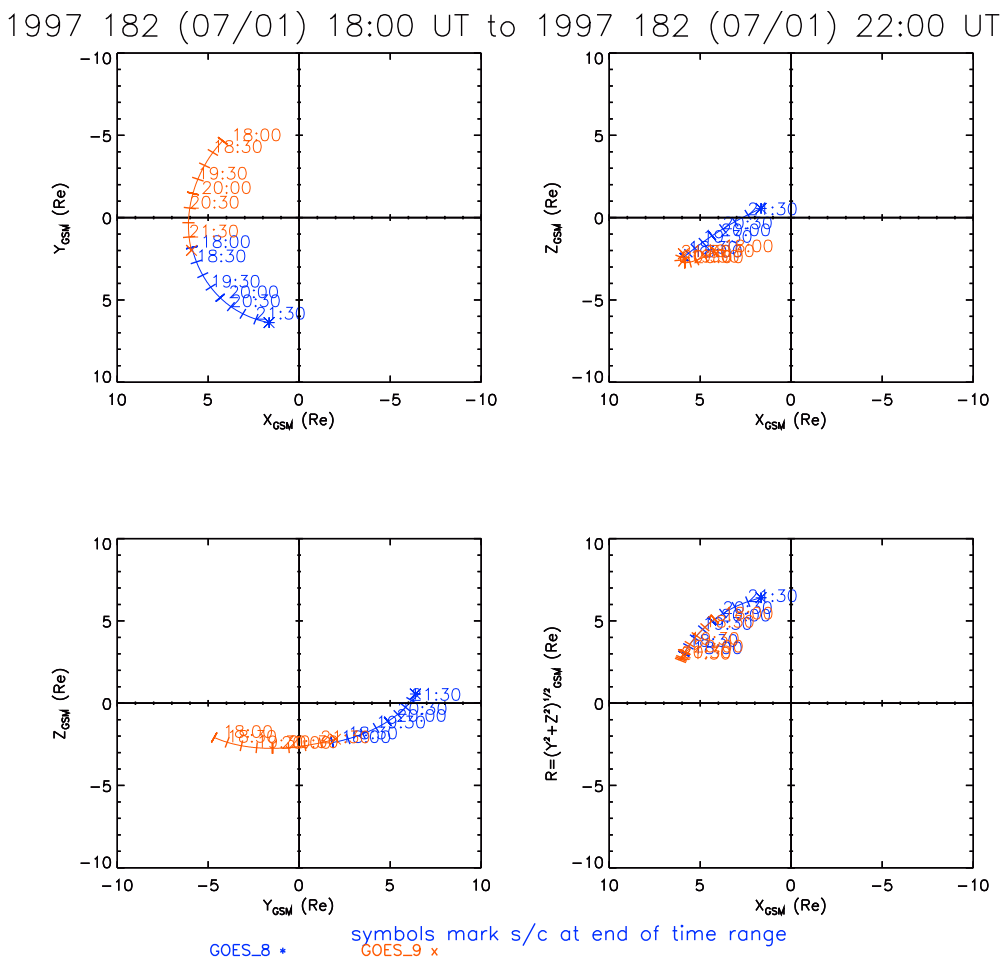

Key Parameter and Survey data (labels K0,K1,K2) are preliminary data. The GSM coordinate system is time varying.
Generated by CDAWeb on: Fri Sep 7 18:45:23 2012

Solar Wind Pressure=2.1nP IMF BZ=0.0nT

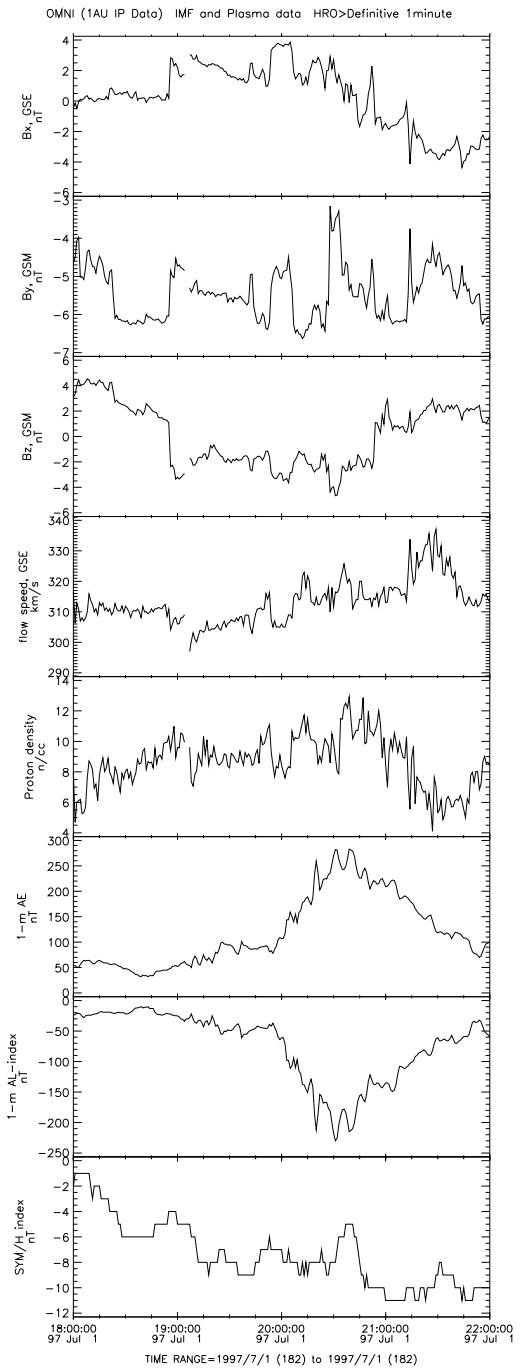

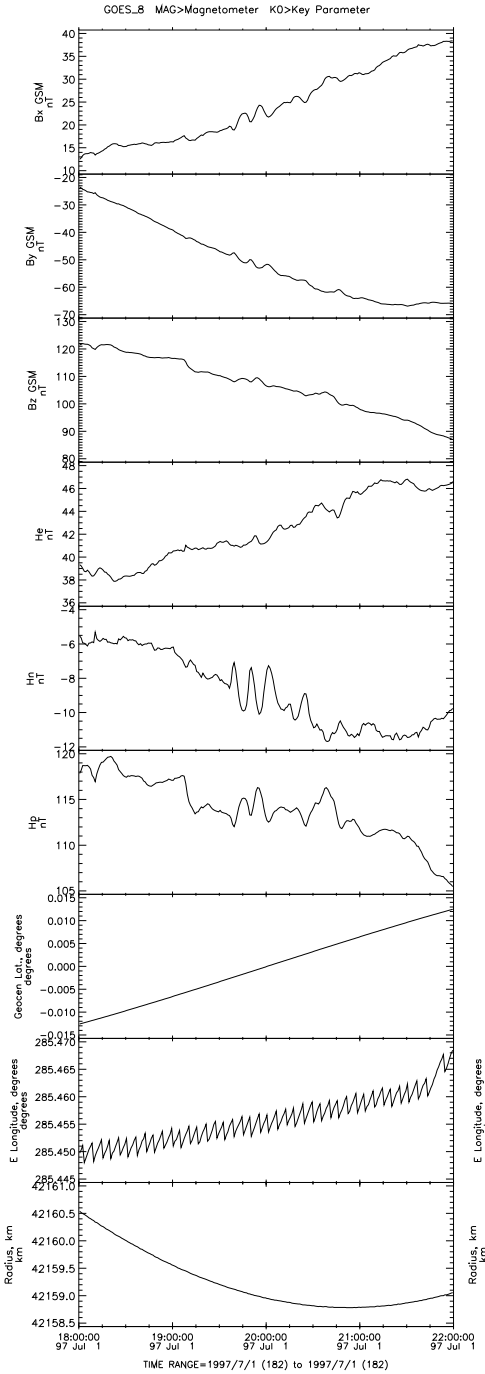

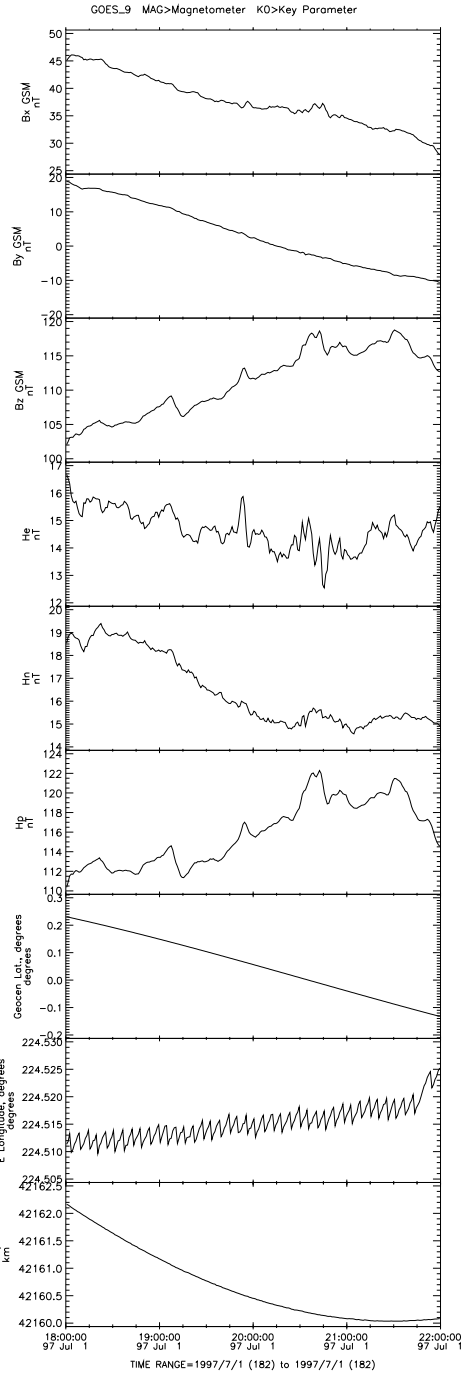

G8 LT = (285 – 360)/15 = UT - 6 hr

G9 LT = (225 – 360)/15 =UT - 9 hr

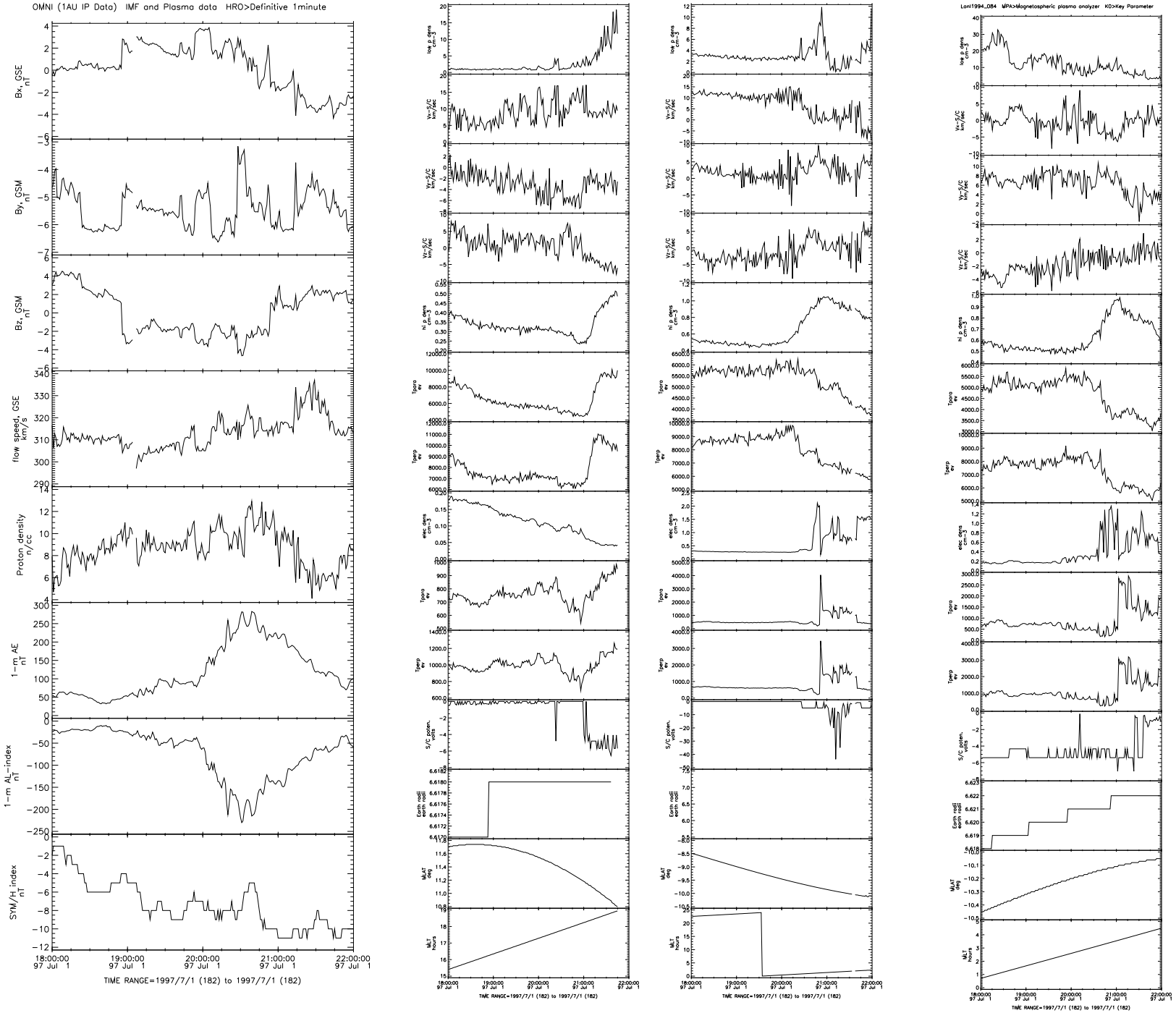
OMNI (1AU IP Data) IMF and Plasma data HRO>Definitive 1minute
Bx, GSE nT
By, GSM nT
Bz, GSM nT
flow speed, GSE km/s
Proton density n/cc
1-m AE nT
1-m AL-index nT
SYM/H index nT
18:00:00 97 Jul 1
19:00:00 97 Jul 1
20:00:00 97 Jul 1
21:00:00 97 Jul 1
22:00:00 97 Jul 1
TIME RANGE=1997/7/1 (182) to 1997/7/1 (182)
Lanl1990_095 MPA>Magnetospheric plasma analyzer KO>Key Parameter
Lanl1991_080 MPA>Magnetospheric plasma analyzer KO>Key Parameter
Lanl1994_084 MPA>Magnetospheric plasma analyzer KO>Key Parameter
low p. dens cm-3
Vx-S/C km/sec
Vy-S/C km/sec
Vz-S/C km/sec
hi p. dens cm-3
Tpara ev
Tperp ev
elec dens cm-3
S/C poten. volts
Earth radii
MLAT deg
MLT hours

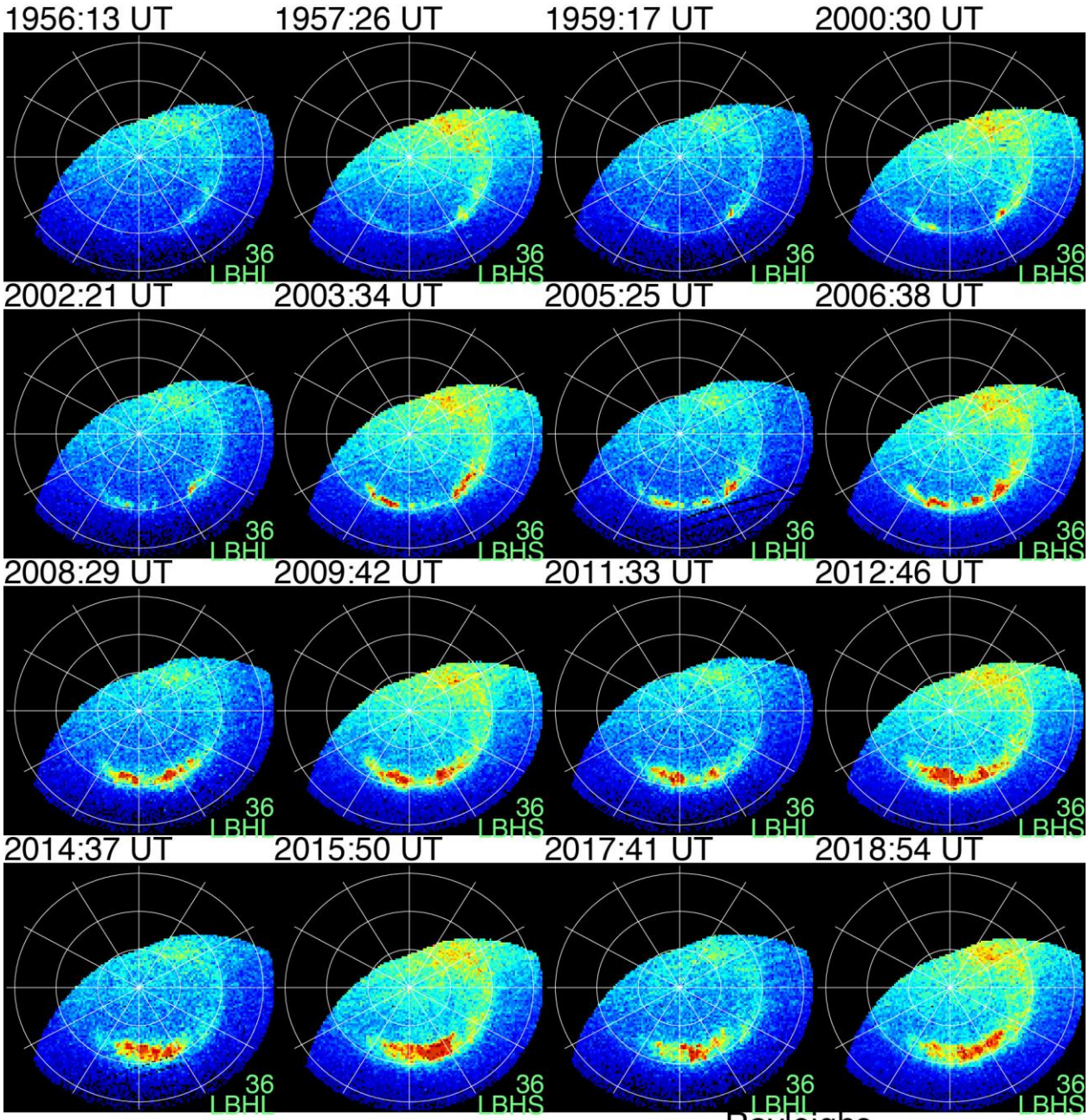
1956:13 UT
1957:26 UT
1959:17 UT
2000:30 UT
2002:21 UT
2003:34 UT
2005:25 UT
2006:38 UT
2008:29 UT
2009:42 UT
2011:33 UT
2012:46 UT
2014:37 UT
2015:50 UT
2017:41 UT
2018:54 UT
36 LBHL
36 LBHS
Ultraviolet Imager/Polar
Day (182) 01 Jul 1997
Rayleighs
0
200
400
600
800
1000
1200

Polar UVI

1996 May 12 21:00 – 24:00 UT

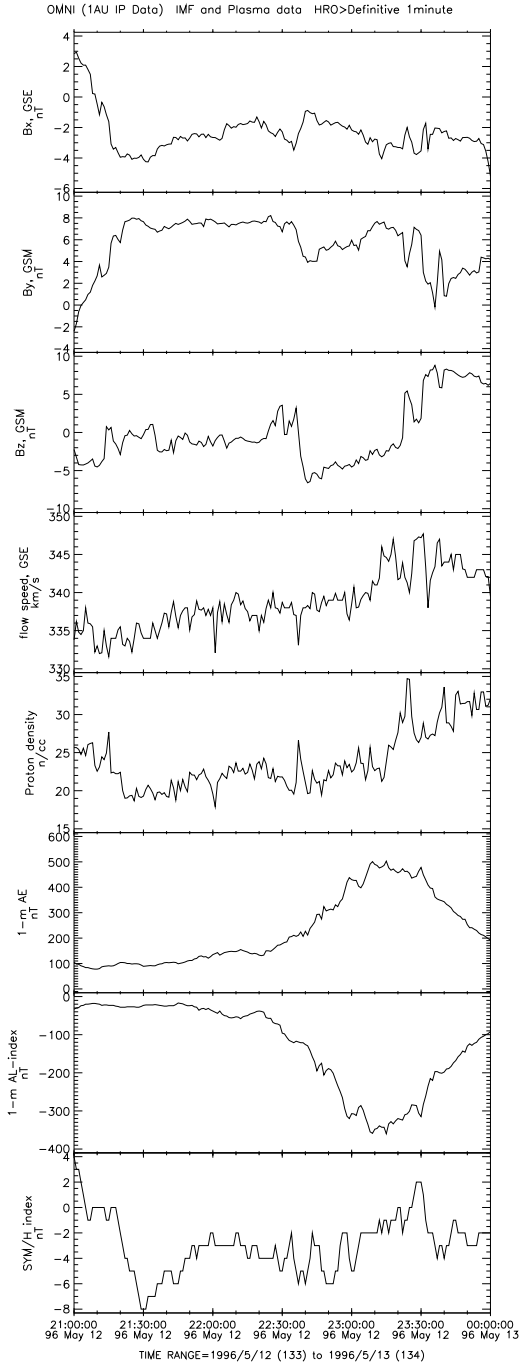

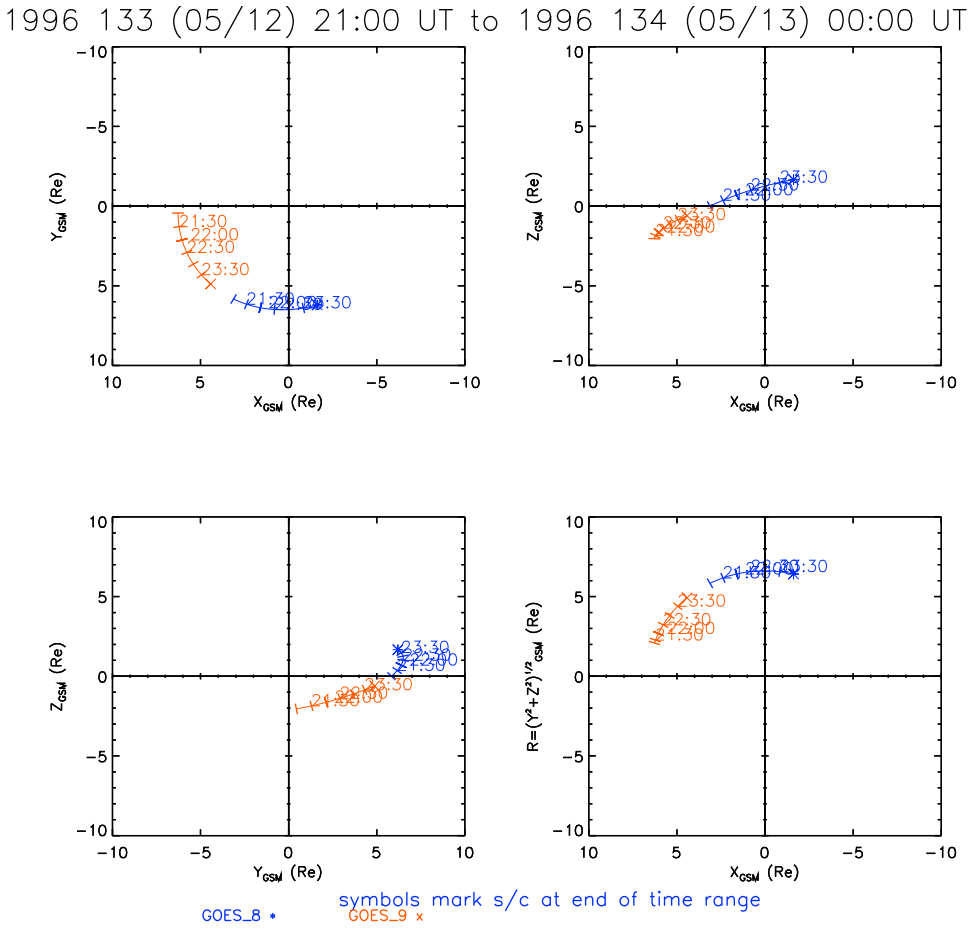

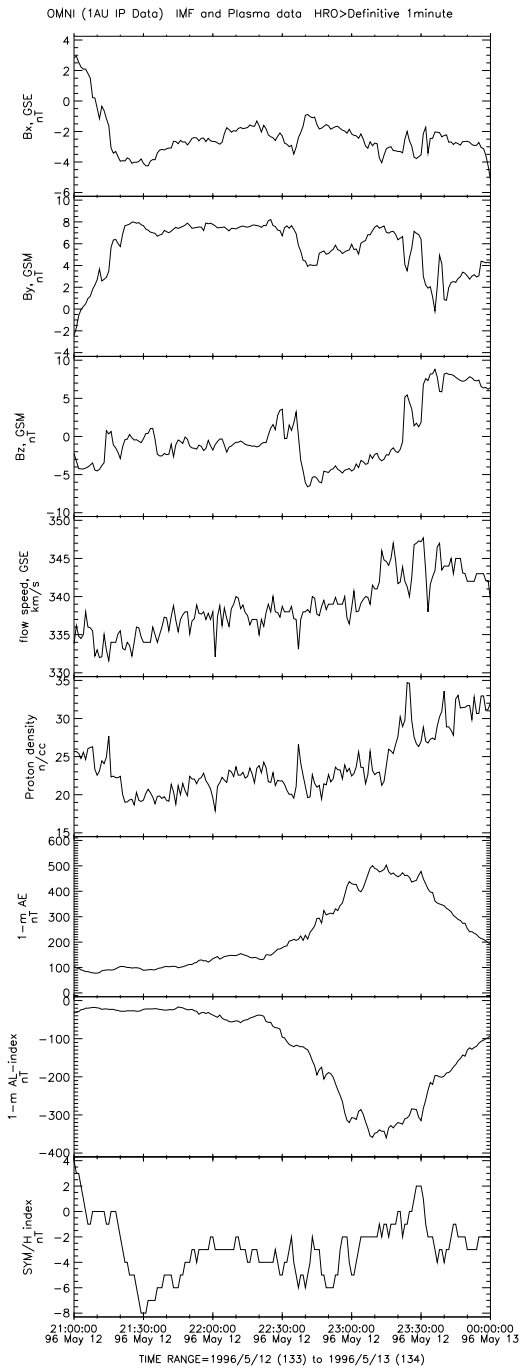

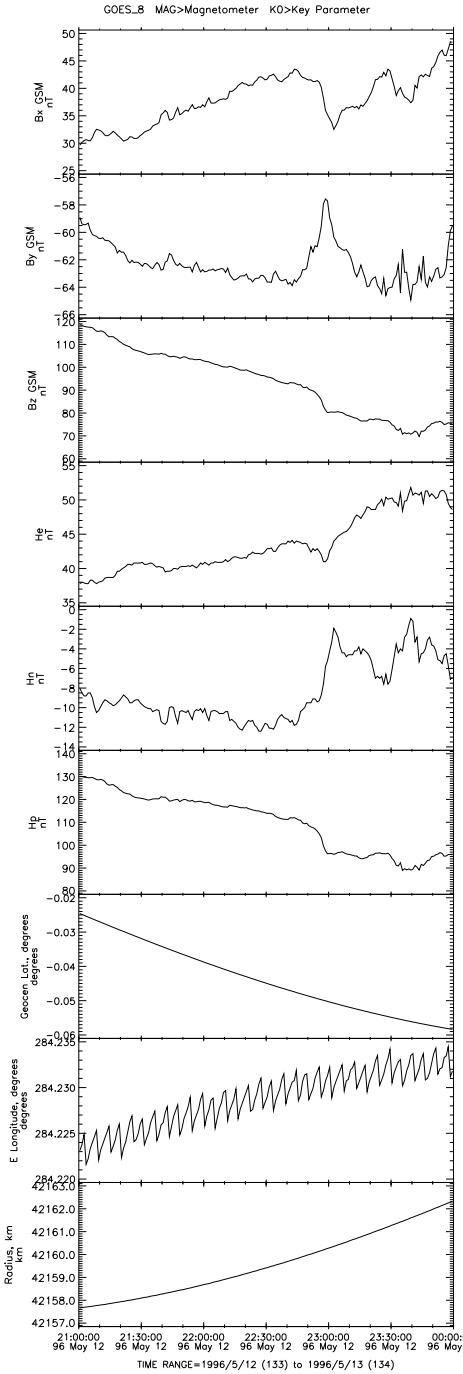

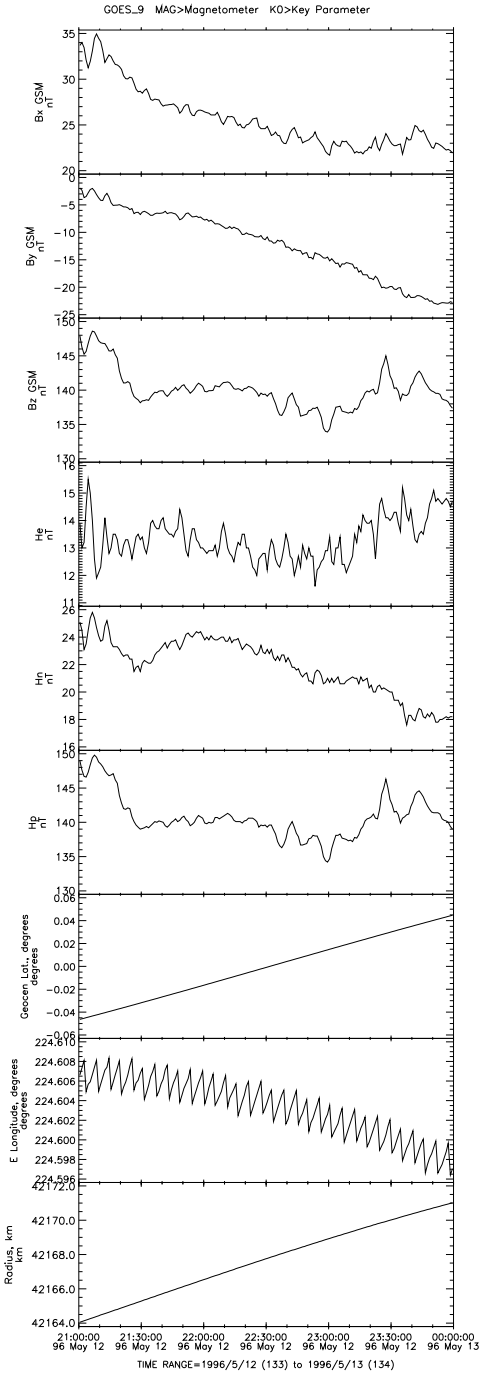

G8 LT = (285 – 360)/15 = UT - 6 hr

G9 LT = (225 – 360)/15 =UT - 9 hr

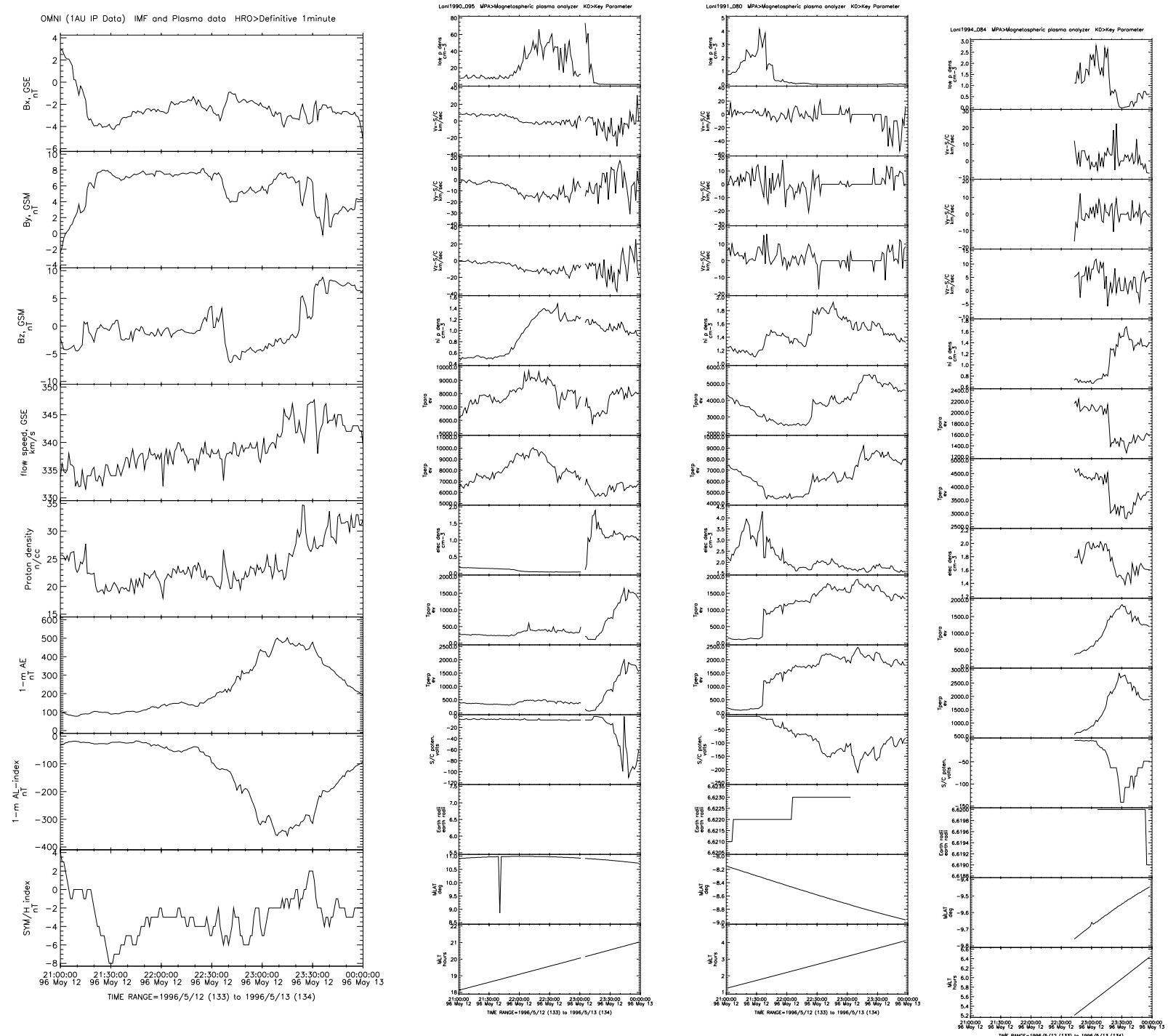
OMNI (1AU IP Data) IMF and Plasma data HRO>Definitive 1minute
Bx, GSE nT
By, GSM nT
Bz, GSM nT
flow speed, GSE km/s
Proton density n/cc
1-m AE nT
1-m AL-index nT
SYM/H index nT
21:00:00 96 May 12
21:30:00 96 May 12
22:00:00 96 May 12
22:30:00 96 May 12
23:00:00 96 May 12
23:30:00 96 May 12
00:00:00 96 May 13
TIME RANGE=1996/5/12 (133) to 1996/5/13 (134)
Lan1990_095 MPA>Magnetospheric plasma analyzer KO>Key Parameter
low p. dens cm-3
Vx-S/C km/sec
Vy-S/C km/sec
Vz-S/C km/sec
hi p. dens cm-3
Tpara ev
Tperp ev
elec. dens cm-3
S/C poten. volts
Earth radii earth radii
MLAT deg
MLT hours
TIME RANGE=1996/5/12 (133) to 1996/5/13 (134)
Lan1991_080 MPA>Magnetospheric plasma analyzer KO>Key Parameter
TIME RANGE=1996/5/12 (133) to 1996/5/13 (134)
Lan1994_084 MPA>Magnetospheric plasma analyzer KO>Key Parameter

Two types of studies

1. Case study: examine carefully a small number of events.
   - investigate how long it takes for the geosynchronous parameter to respond to changes in the solar wind
2. Statistical study: examine a large number of events
   - least square fit of solar wind dynamic pressure vs. geosynchrnous Bz

- Geosynchronous satellites can provide rich datasets for space weather and space physics
- Could we get the next generation Palapa satellite to provide magnetic field and other scientific data?

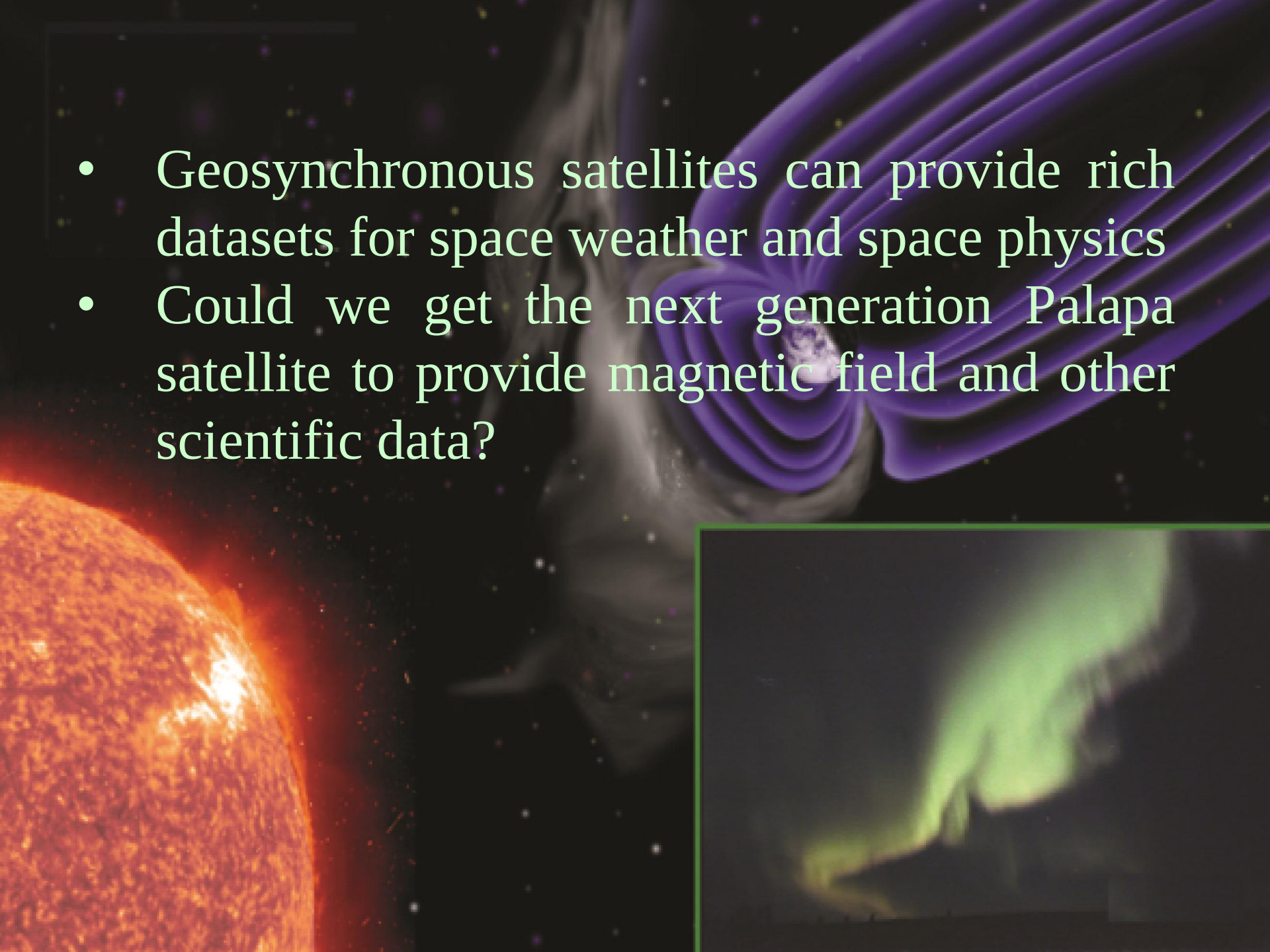

4. A space weather tool: Neural networks

a. **HF backscatters from ionospheric irregularities**
b. **Kp forecast models**

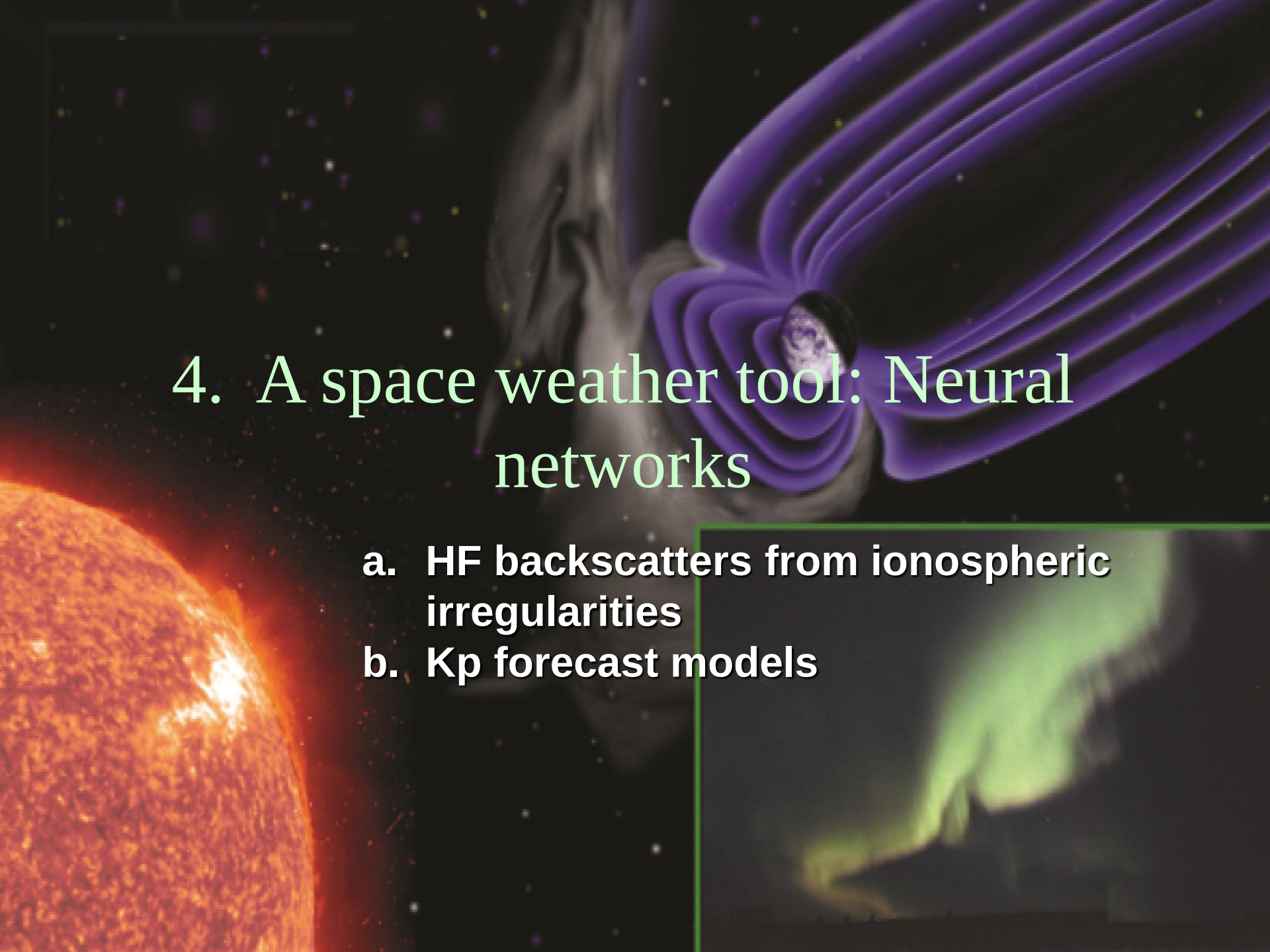

The underlying physics of many space objects and phenomena is often complex and not well understood, but progress can be achieved through the use of advanced or even standard machine learning and artificial intelligence principles

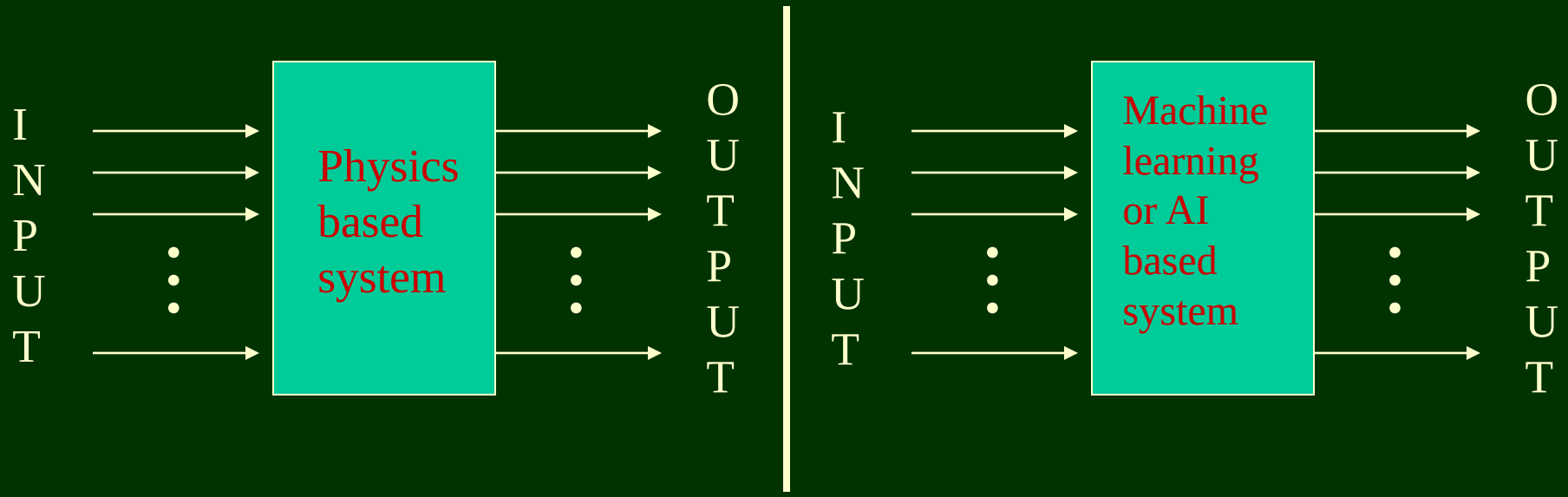

Neural Networks

- A NN architecture with 1 hidden layer [a class of multi-layer feedforward network (MLFN)]

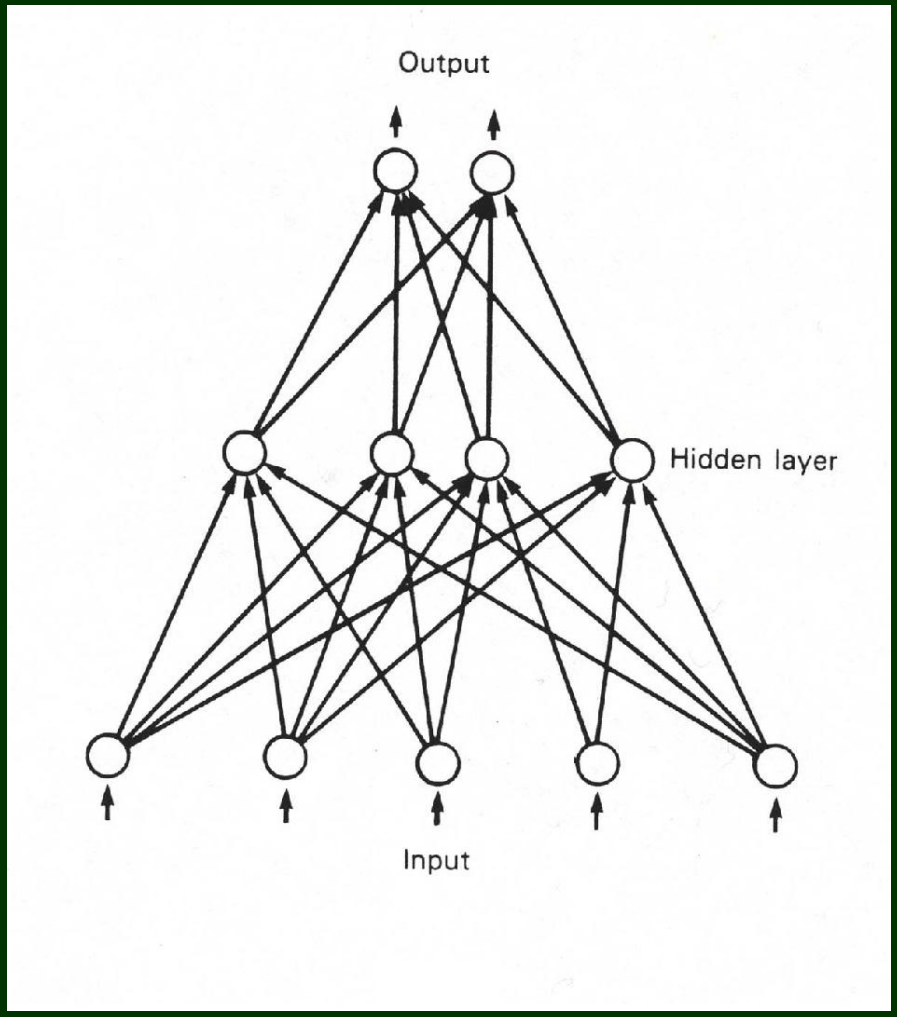

The intelligence lies in the connections between the nodes

A class of NN with 0 hidden layer is called perceptron

Neural Network algorithm

Feed forward step

Let $I_i^{(p)}$ denote the i-th element of the p-th input vector; $w_{ji}^{(1)}$ the weight (strength) between the j-th node of the hidden layer (layer 1) and the i-th node of the input layer (layer 0). The corresponding weight for the connection between the hidden layer and the output layer (layer 2) will be denoted by $w_{ji}^{(2)}$.

For a given input vector $I^{(p)} = (I_1^{(p)} ..., I_{n_i}^{(p)})$ the output vector of the input units is given by the vector $O^{(p,0)} = I^{(p)}$. Here n_i is the number of input units and the superscript 0 in (p,0) serves to denote that this is output from level 0. The input $I_j^{(p,1)}$ to the j-th node of the hidden layer (level 1) is given by

$$I_j^{(p,1)} = \sum_{i=1}^{n_i} w_{ji}^{(1)} O_i^{(p,0)} \quad (3)$$

The processing units in the networks used in this s tudy compute their output by applying a sigmodial or logistic function, f, to their input:

$$f(x) = \frac{1}{1+e^{-x}} \quad (4)$$

In addition, all hidden and output units have associated with them biases which modulate the sensitivity of the unit to its input. Thus the output $O_j^{(p,1)}$ of the j-th hidden node is given by

$$O_j^{(p,1)} = \frac{1}{1+e^{-\left(I_j^{(p,1)} + b_j^{(1)}\right)}} \quad (5)$$

where $b_j^{(1)}$ is the bias of the j-th hidden node. We note that the bias term can be interpreted as the weight of a connection between a virtual input node which is always "on" (and is usually called the true node) and the j-th unit. Thus the bias is just another learnable weight.

Similarly, the input and output of the j-th unit of the output layer (level 2) are

Neural Network algorithm

Feed forward step

Similarly, the input and output of the j-th unit of the output layer (level 2) are

$$I_j^{(p,2)} = \sum_{i=1}^{n_h} w_{ji}^{(2)} O_i^{(p,1)} \quad (6)$$

and

$$O_j^{(p,2)} = \frac{1}{1+e^{-\left(I_j^{(p,2)} + b_j^{(2)}\right)}} \quad (7)$$

where n_h is the number of units in the hidden layer. This completes the forward pass for the input vector $I^{(p)}$.

Neural Network algorithm

Back-propagation step

We want to minimize the total error

$$E = \sum_{p=1}^{n_p} E^p = \frac{1}{2}\sum_{p=1}^{n_p}\sum_{j=1}^{n_o}\left(T_j^{(p)} - O_j^{(p,2)}\right)^2 \quad (8)$$

where n_o is the number of output vectors.

Using Eqs. (6) and (7) in (8) we see that E is a function of the $w_{ji}^{(2)}$ and differentiating E with respect to $w_{ji}^{(2)}$ gives

$$\frac{\partial E}{\partial w_{ji}^{(2)}} = -\sum_{p=1}^{n_p}\left(T_j^{(p)} - O_j^{(p,2)}\right)O_j^{(p,2)}\left(1 - O_j^{(p,2)}\right)O_i^{(p,1)} = -\sum_{p=1}^{n_p}\delta_j^{(p,2)}O_i^{(p,1)} \quad (9)$$

where we have used the fact that $f'(x) = f(x)(1 - f(x))$ and we define $\delta_j^{(p,2)}$ to be

$$\delta_j^{(p,2)} = \left(T_j^{(p)} - O_j^{(p,2)}\right)O_j^{(p,2)}\left(1 - O_j^{(p,2)}\right) \quad (10)$$

Since the gradient is the direction of the maximum rate we wish to move in the opposite direction

so that the equation of the weight change, $\Delta w_{ji}^{(2)}$ is

$$\Delta w_{ji}^{(2)} = \eta\sum_{p=1}^{n_p}\delta_j^{(p,2)}O_i^{(p,1)} \quad (11)$$

where η is a learning rate parameter. Thus the expression for the weight $w_{ji}^{(2)}$ at the $(t+1)^{-st}$ presentation of the set of training vectors is given by

$$W_{ji}^{(2)}(t+1) = w_{ji}^{(2)}(t) + \eta\sum_{p=1}^{n_p}\delta_j^{(p,2)}O_i^{(p,1)} + \alpha\Delta w_{ji}^{(2)}(t) \quad (12)$$

In Eq. (12), the last term is a momentum term which enhances the stability of the computations

Neural Network algorithm

Back-propagation step

In Eq. (12), the last term is a momentum term which enhances the stability of the computations by suppressing high frequency fluctuations in the weights.

The dependence of E on the $w_{ji}^{(2)}$ is more complicated but easily expressed using Eqs. (3), (5–8). From these we find that

$$\frac{\partial E}{\partial w_{ji}^{(1)}} = -\sum_{p=1}^{n_p} \delta_j^{(p,1)} O_i^{(p,0)} \tag{13}$$

where

$$\delta_j^{(p,1)} = O_j^{(p,1)}\left(1 - O_j^{(p,1)}\right)\sum_{m=1}^{n_o} \delta_m^{(p,2)} w_{mj}^{(2)} \tag{14}$$

Thus the equation for the new value of w_{ji} is

$$w_{ji}^{(1)}(t+1) = w_{ji}^{(1)}(t) + \eta \sum_{p=1}^{n_p} \delta_j^{(p,1)} O_i^{(p,0)} + \alpha \Delta w_{ji}^{(1)}(t) \tag{15}$$

Two applications of neural networks

a. HF backscatters from ionospheric irregularities (clutters)
b. Kp forecast models

Could NN be used to predict spacecraft charging and other parameters/phenomena at geosynchronous orbit?

4.a HF backscatters from ionospheric irregularities (clutters)

Johns Hopkins Goose Bay HF radar

Goose Bay high-frequency (HF) radar:

- operated by the Johns Hopkins University Applied Physics Lab
- study the ionosphere E and F layers, 100 – 500 km in altitude
- radar descriptions/characteristics [Greenwald et al., 1985]:
  - Operating frequencies: 8 – 20 MHz
  - 16 log-periodic antennas that are electronically steerable
  - 16 beams with each beam typically consisting of 75 ranges
  - Detects backscattered signals from ionospheric irregularities or clutter ("soft target")
  - Backscattered signal is proportional to n^2 [Walker et al., 1987]

Goose Bay HF radar

- Goose Bay HF radar is part of the worldwide SuperDARN radar network [Greenwald et al., 1995]

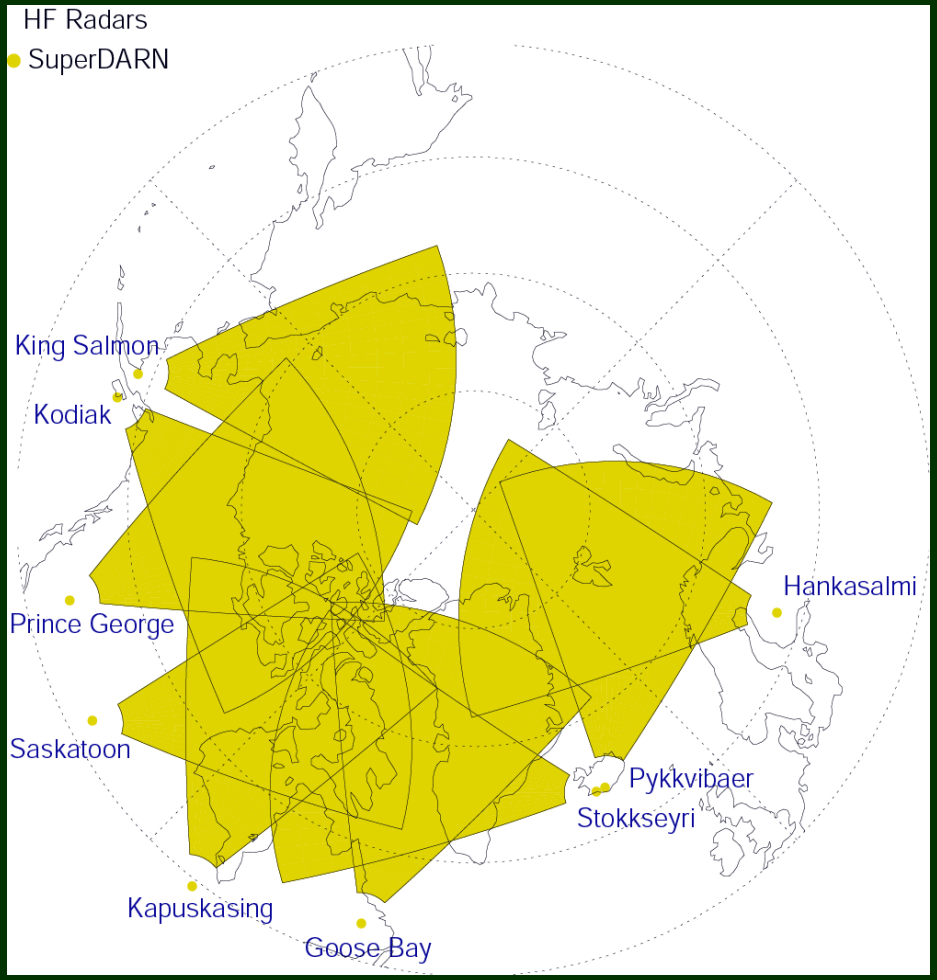

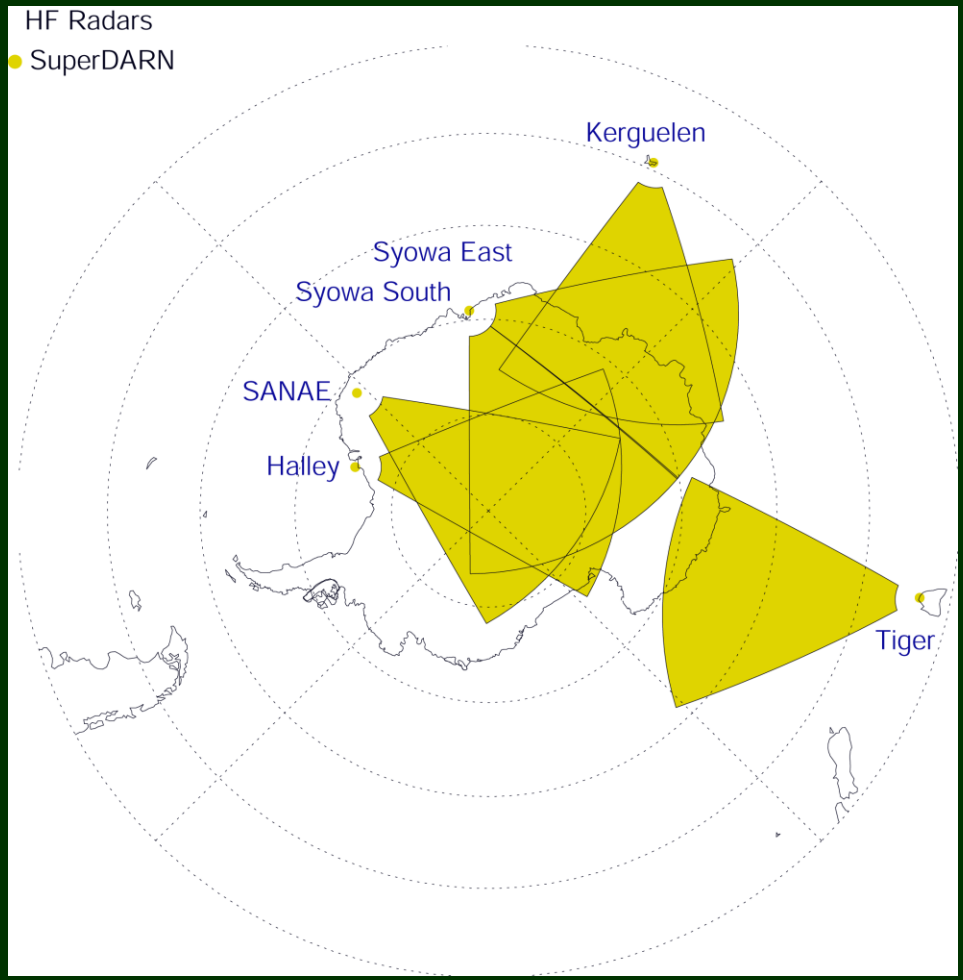

Halley Bay, Antartica

Kapuskasing, Ontario, Canada

Stokkseyri, Iceland

Goose Bay HF radar

- One of the most popular products of the SuperDARN radars is the ionospheric convection pattern

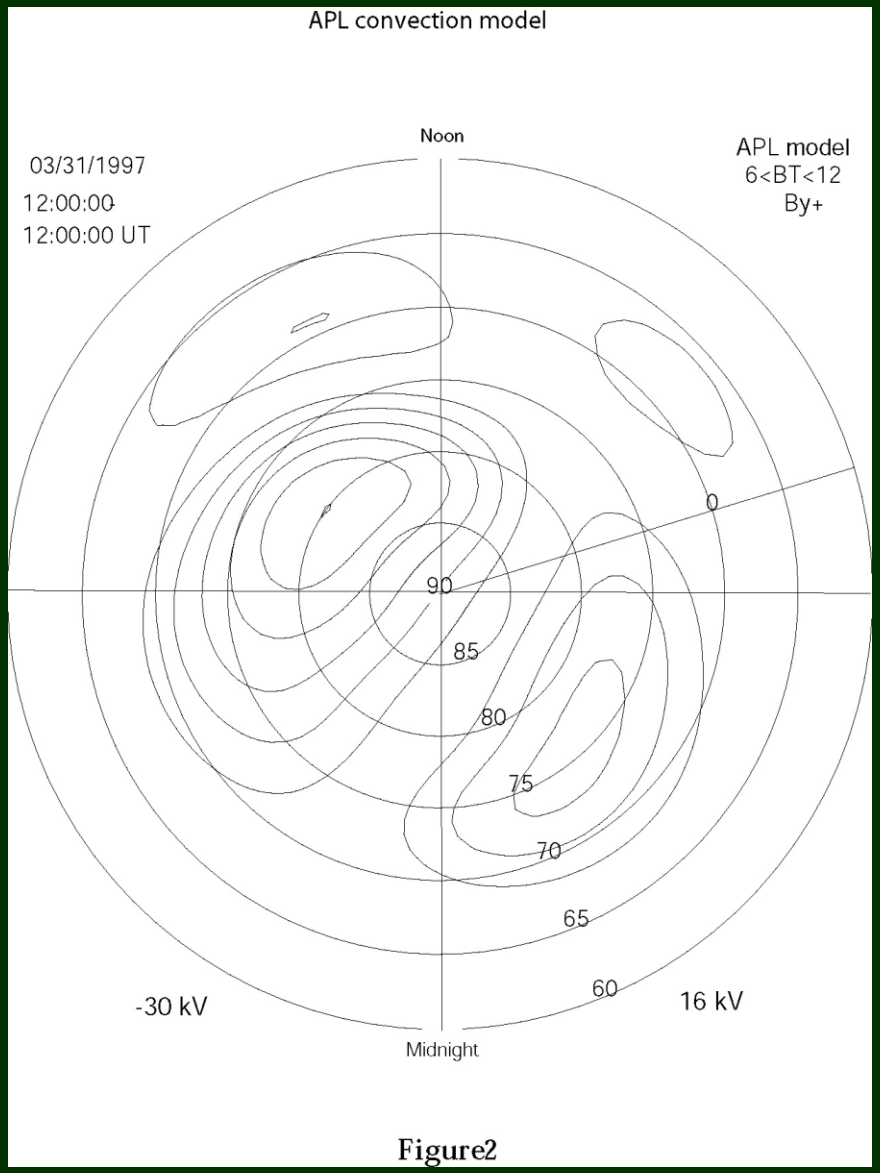

Figure2

Goose Bay HF radar analysis

- A lot of processing is required to get from the raw radar signals to the finished products, e.g. ionospheric convection patterns
- The radar uses a multi-pulse technique to determine a complex autocorrelation function (ACF) at each range gate [Farley, 1972; Greenwald et al., 1985]
- Processing ACFs could take a lot of time, especially in the early days when computers were slow
- From these ACFs, several parameters can be extracted to derive physically important quantities
- For example, ACFs => Doppler velocity => convection patterns

ACF

Examples of usable and unusable ACFs

—— = real

------- = imaginary

Wing et al. [2003]

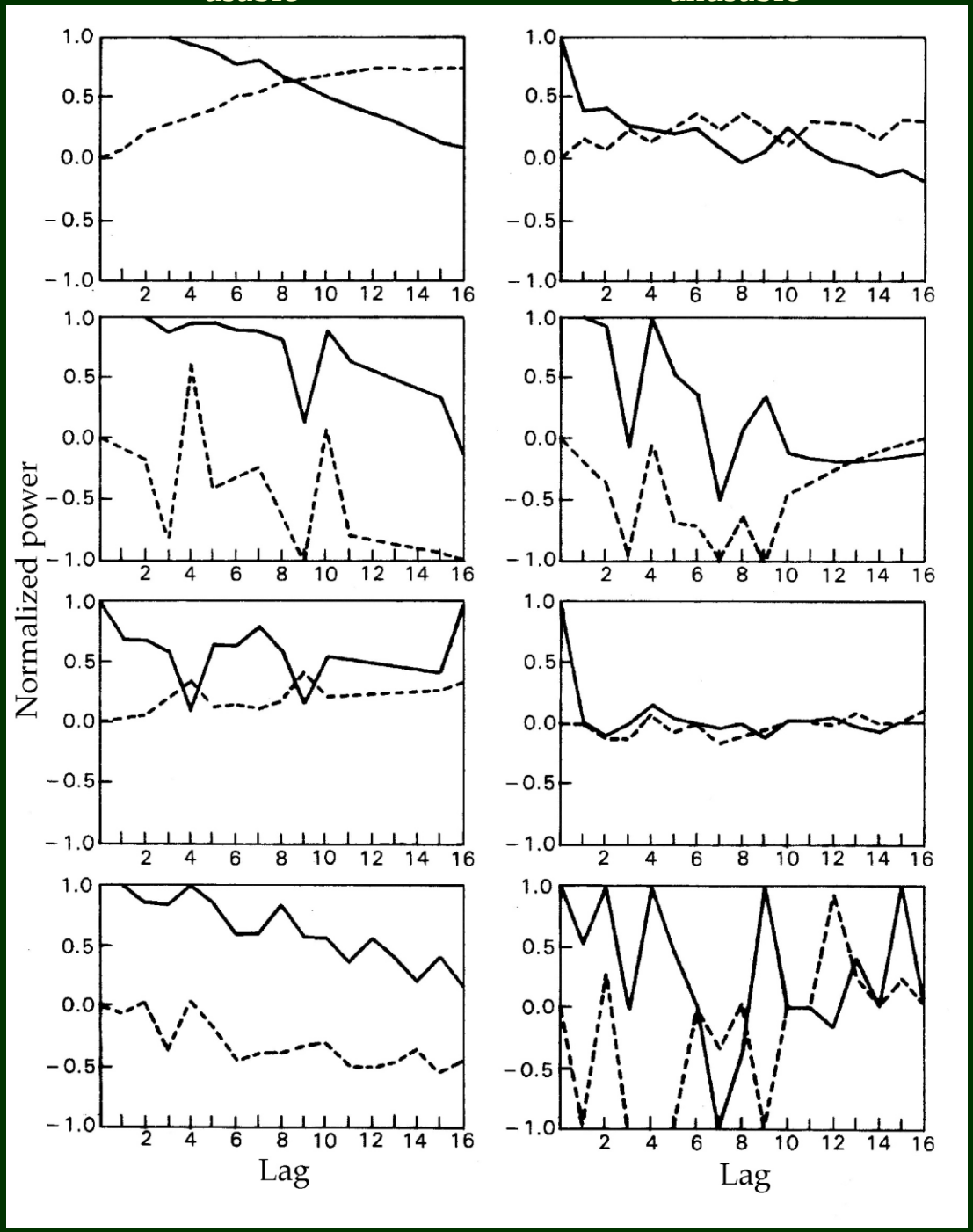

objective

- A proof-of-concept study to investigate the capability of NNs to classify usable and unusable ACFs

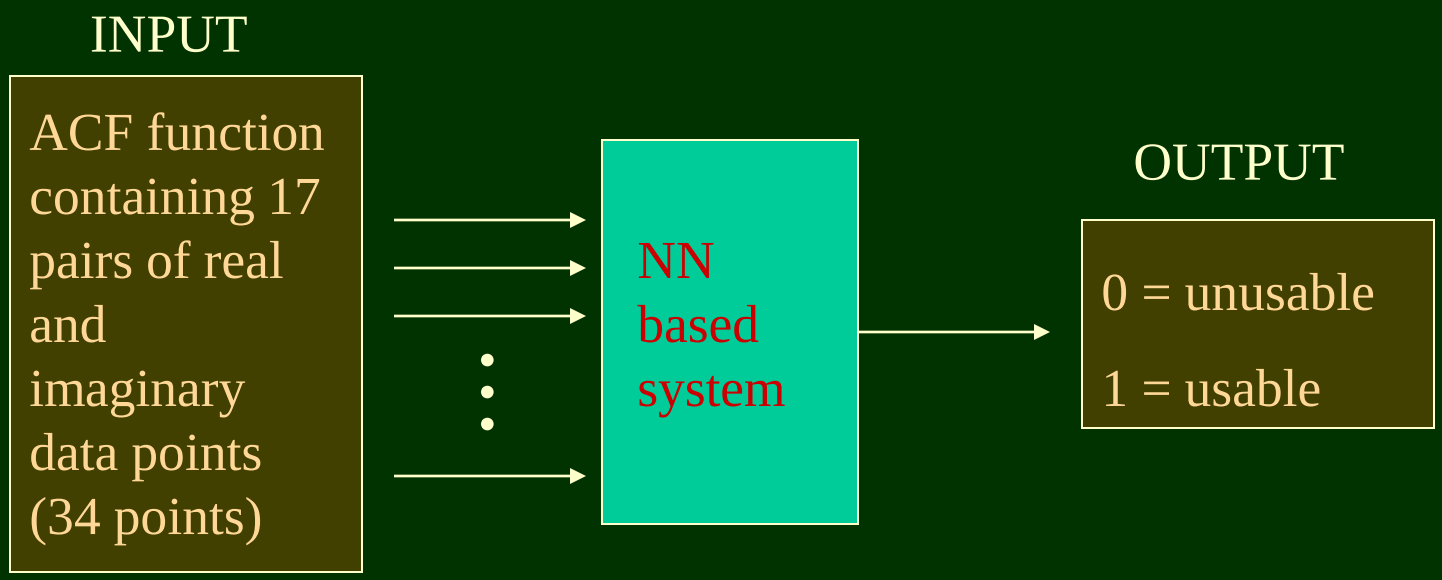

Data set

- 350 ACFs from Goose Bay radar database 1986-1987
- 200 ACFs randomly selected for the training data set and 150 for the test data set
- Each ACF contains 17 pairs of real and imaginary data points (M=17), which are the inputs to NN

The dataset has been widely distributed and is known as the Johns Hopkins ionosphere radar dataset in the machine learning community

Results

Examined the following NN architectures:

- MLFN - NNs with 1 hidden layer and 3, 5, 8, 10, and 15 hidden nodes
- Perceptrons - (NNs with 0 hidden layer): linear and non-linear

Wing et al. [2003]

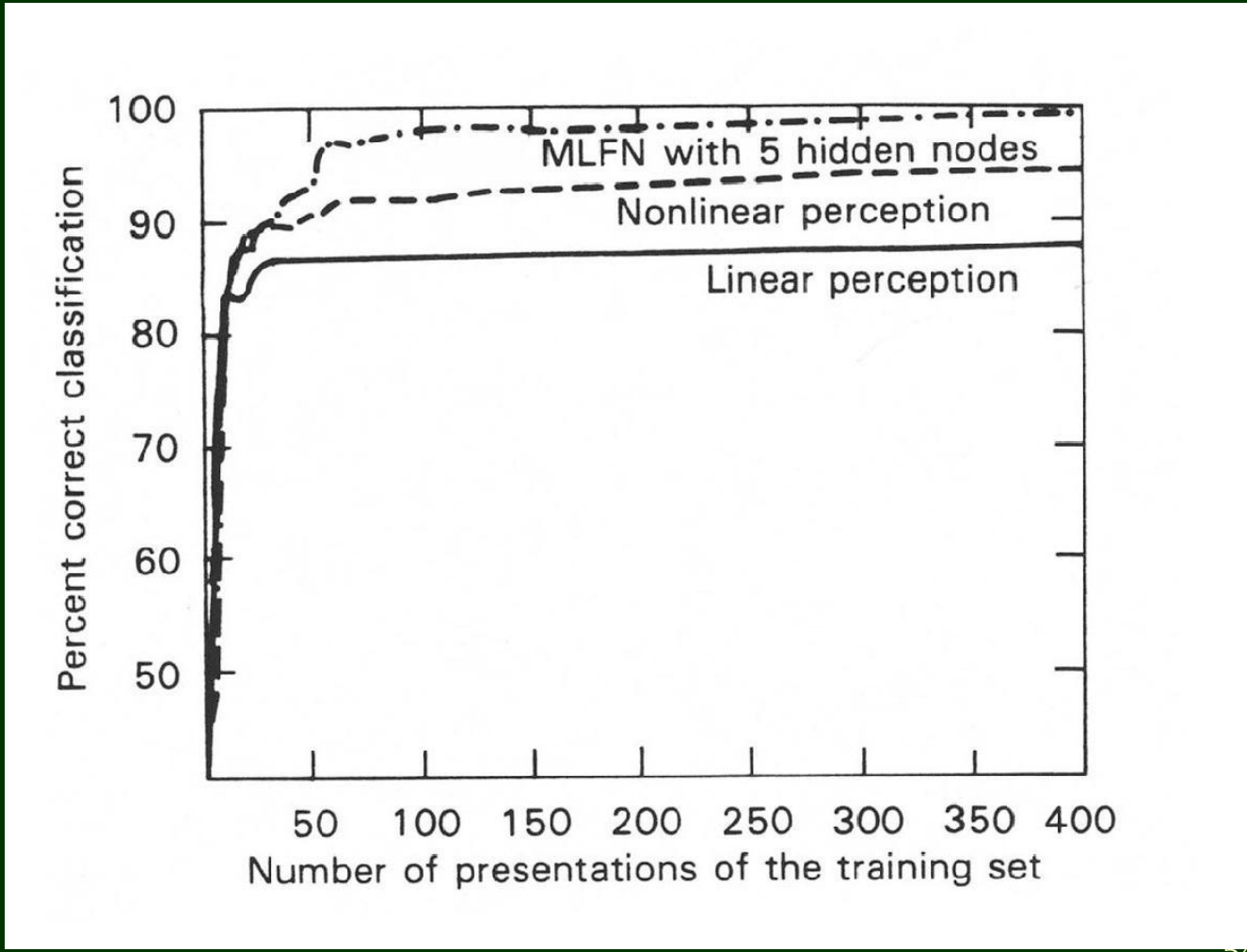

NN learning curve

4.b Kp forecast models

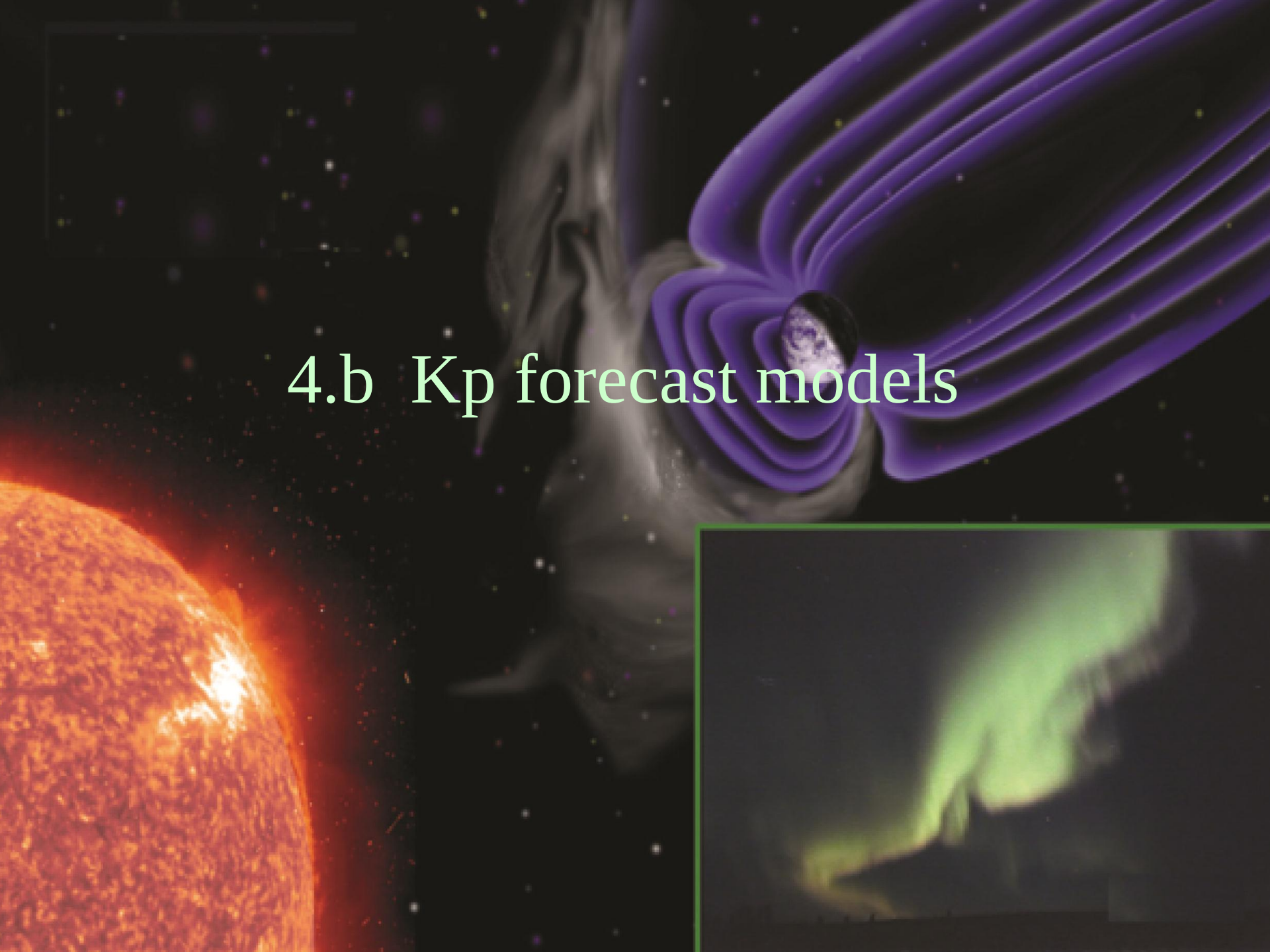

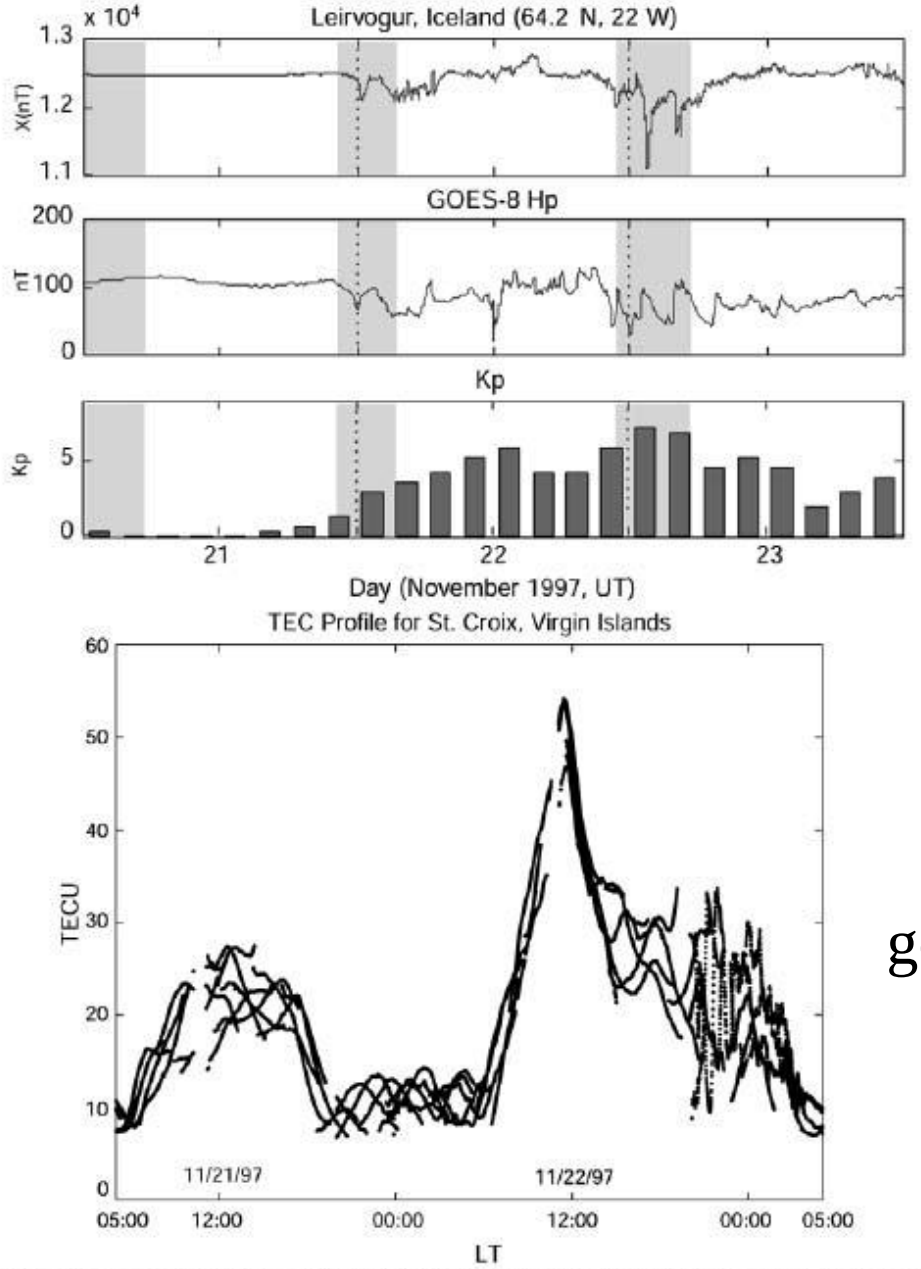

Figure 1. The top three panels show, respectively, the pole-ward component of the magnetic field, measured at Leirvogur, Iceland (top); data from the fluxgate magnetometer on the geostationary satellite GOES-8, which is located at 75° W longitude (middle); Kp indices for the same period. The bottom panel shows the total equivalent vertical electron content (1 TECU = 10^{16} m^{-2}) for all GPS satellites in view from St. Croix near Puerto Rico on November 21-22, 1997; LT = UT – 4 hours [after *Kelley et al., 2000*].

Bhattacharyya and Basu [2002]

geographic lat = 18 deg N

Pandey and Dashora [2005]

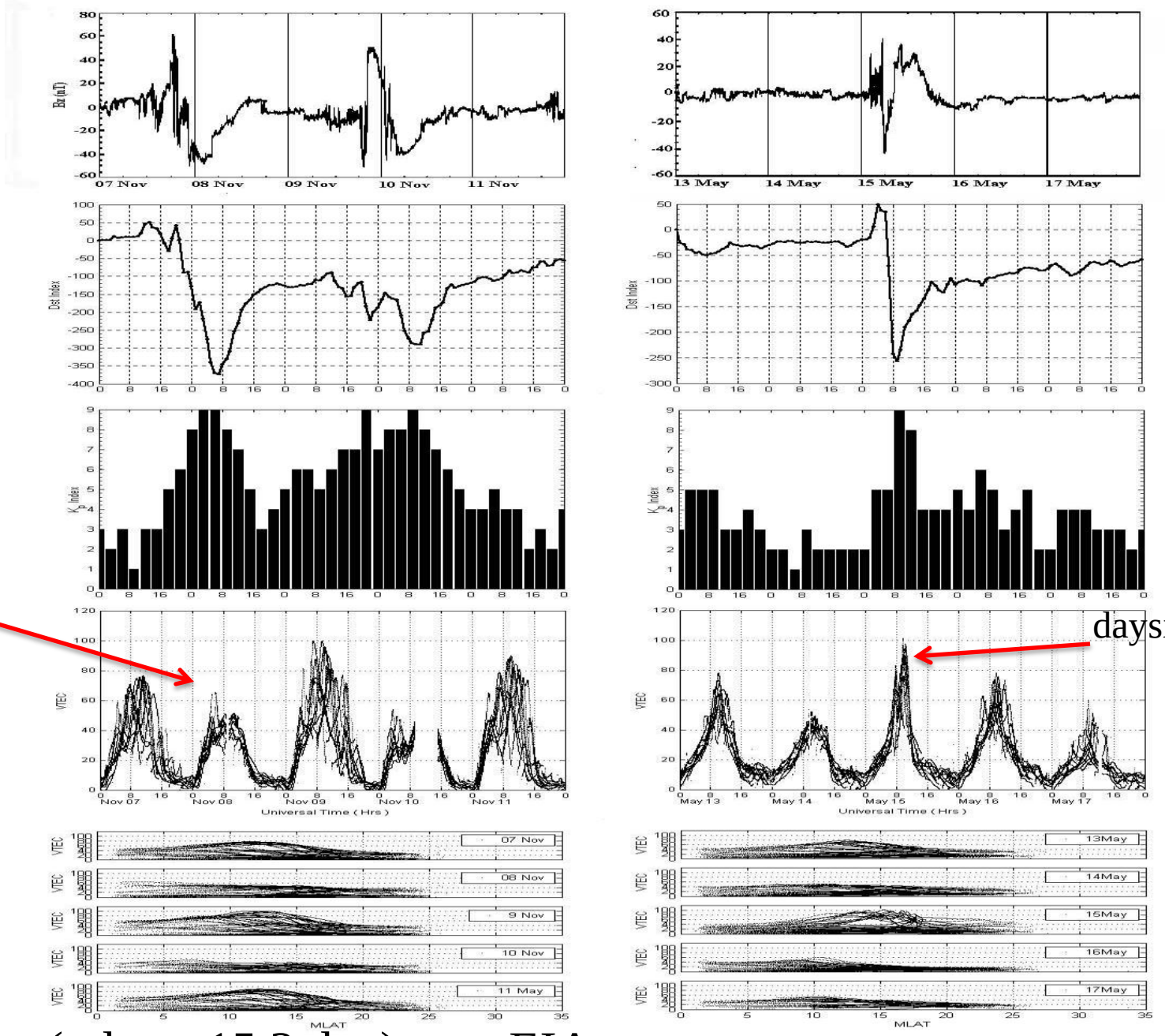

Udaipur (mlat = 15.3 deg) near EIA

Background and Motivations for developing Kp forecast models

- Moderate and high activities are notoriously difficult to predict [Joselyn, 1995].
- Real-time magnetometer data can be used to calculate nowcast Kps, which could improve the accuracy of the forecast Kps.

Why Kp?

- Kp is one of the most popular global indices.
- Kp has been playing significant roles in space weather, e.g., satellite drags, satellite communication, etc.
- Many magnetospheric and ionospheric models require Kp as an input parameter, e.g., T89 magnetic field model, Fok ring current-radiation belt model, MSFM, OVATION, etc.
- The long uninterrupted Kp record since 1932 makes it ideal for studying solar-wind magnetosphere interactions, e.g., the solar cycle effects, etc.

The APL Kp forecast models

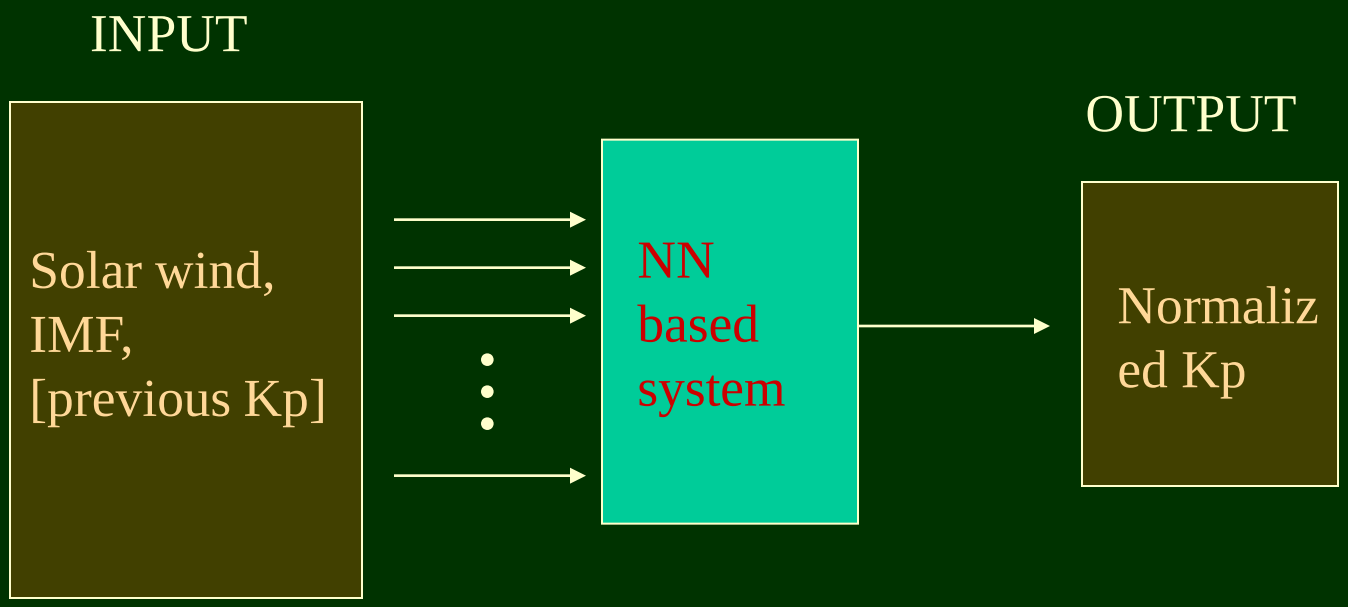

Summary and Conclusion

- In order to satisfy different needs and operational constraints, we developed 3 Kp forecast models:
  1. APL model 1
     - Input: ACE solar wind n, Vx, IMF |B|, Bz, and nowcast Kp
     - Output: ~1-hr ahead Kp forecast
  2. APL model 2
     - Input: same as model 1
     - Output: ~4-hr ahead Kp forecast
  3. APL model 3
     - Input: ACE solar wind n, Vx, IMF |B|, and Bz
     - Output: ~1-hr ahead Kp forecast

- Note: a very accurate nowcast Kp algorithm [Takahashi et al., 2001] can be used as an input to APL models 1 and 2.

Summary and Conclusion

Operational at NOAA/AF

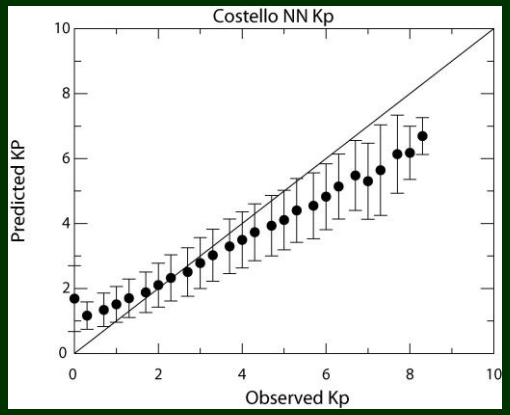

Univ. of Sheffield

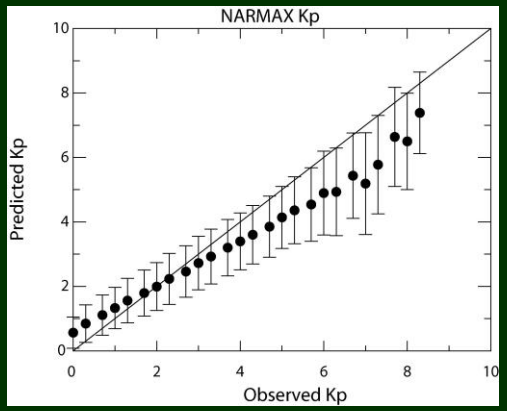

Boberg et al. [2000]
Operational at Lund Obs.

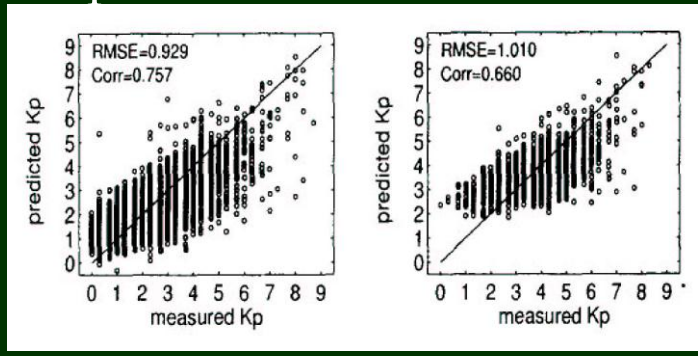

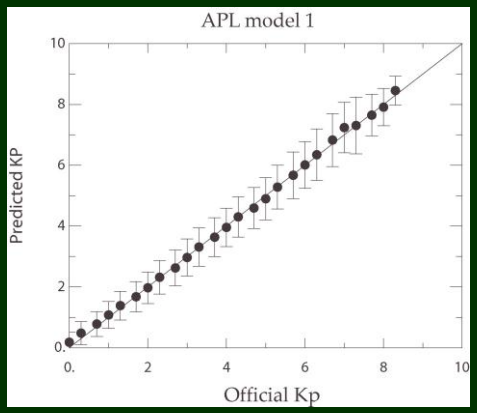

APL model 1

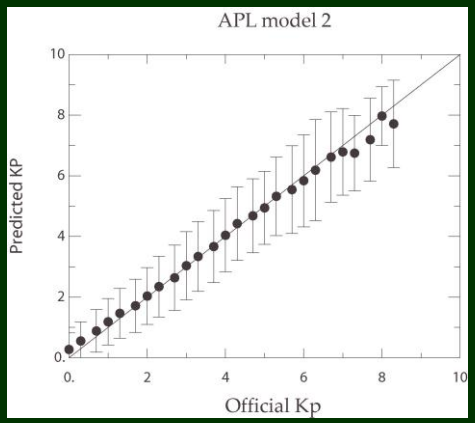

APL model 2
(4 hr ahead
forecast)

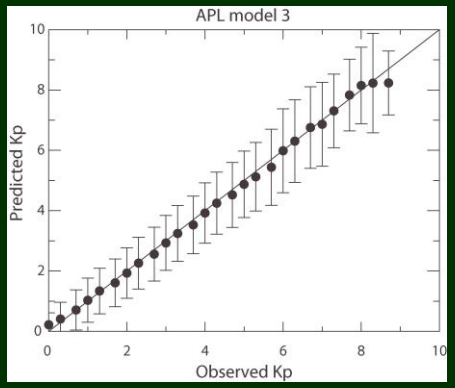

APL model 3
(purely
driven by
solar wind)

Wing et al. [2005]

Predictive Model Performance

The skill scores are defined below (Detman and Joselyn, 1999).

The figures show the skill scores for Costello Neural Network (NN) model over 2 solar cycle periods. They show that the model performance has a solar cycle variation. The model performs better near solarmax than solarmin for active times (Kp > 3). The input parameters to the model are: solar wind V, IMF |B|, IMF Bz, and the previous Kp predictions of the model.

The skill scores are defined below (Detman and Joselyn, 1999).

Forecast

Observed

	Y	N
Y	x	y
N	w	z

True Skill Statistics (TSS):

$$TSS = \frac{xw - yz}{(x+y)(z+w)}$$

Gilbert Skill (GS):

$$GS = \frac{x - Ch}{(x - Ch) + y + z}$$

GS ignores w ("correct rejection").
Ch = chance hits = (probability of Y events to occur) X (number of Y events forecasted)

$$Ch = \frac{(x+y)}{(x+y+z+w)}(x+z)$$

For TSS and GS:
Perfect forcecast = 1
Random forecast = 0

Summary and Conclusion

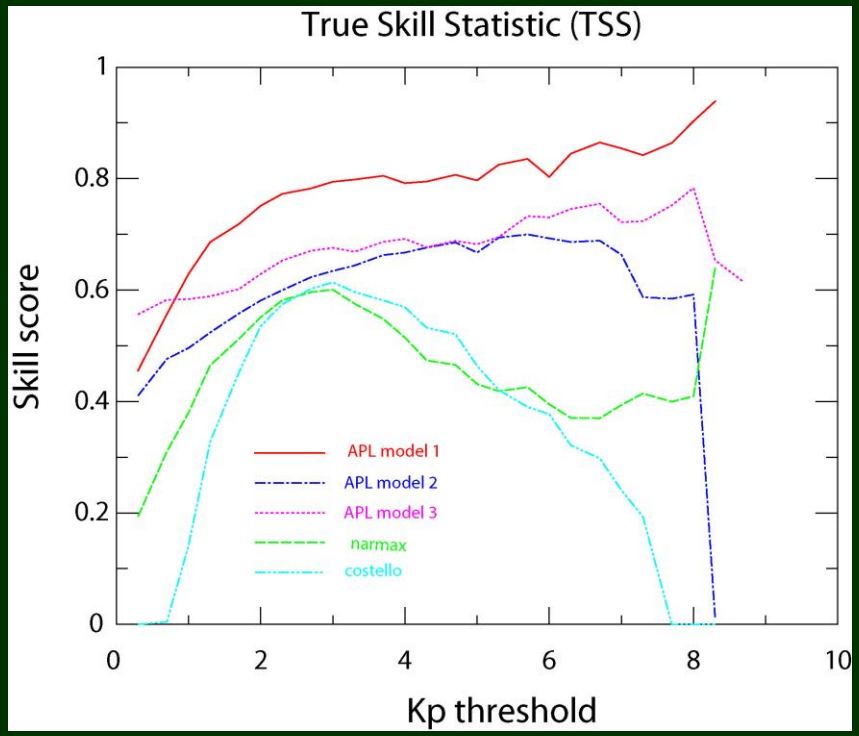

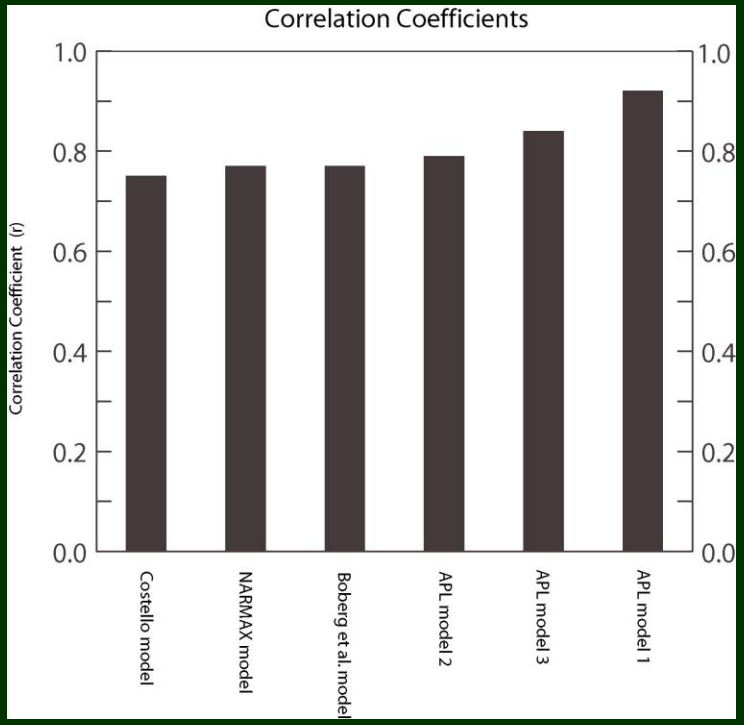

True Skill Statistic (TSS) [Detman and Joselyn, 1999] based on data spanning over 2 solar cycles.

Wing et al. [2005]

Note: for comparisons with other published results, r is calculated over all Kp ranges and therefore, this figure understates the dramatic improvements the APL Kp models obtain for active times, Kp > 4.

NOAA / Space Weather Prediction Center

Predicted Geomagnetic Activity Index
using Wing Kp Model -- 12-hour Plot

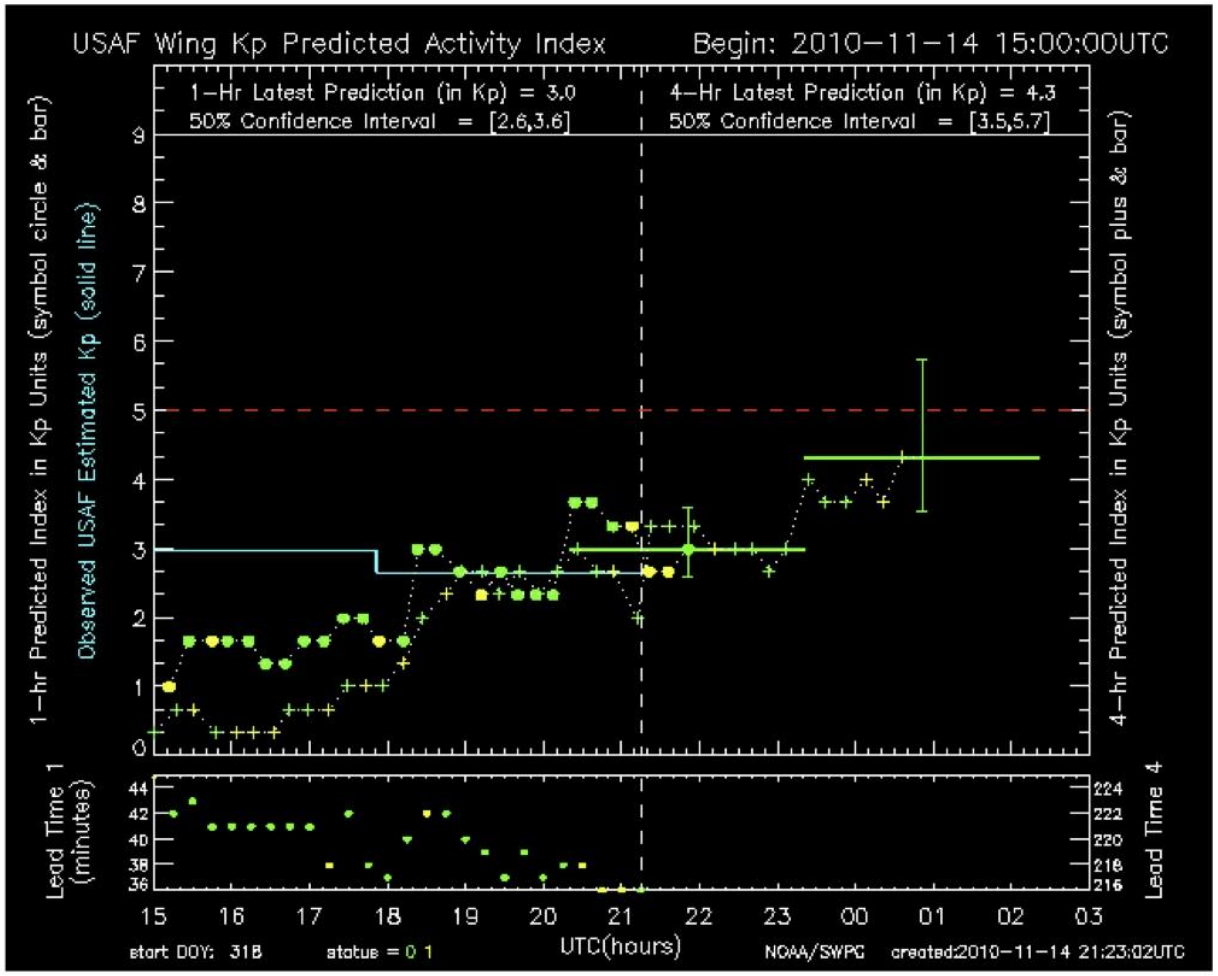

12-hour Plot -- 24-hour Plot -- ASCII list of model output -- 7 Day Model Performance

Predictions update every 15 minutes

5. Summary

- Geosynchronous orbit environment is relevant for many satellites, including Palapa
- Geosynchronous orbit:
  - attractive place to put a satellite
    - stable – save fuel
    - fixed geographical area coverage
  - has space weather risks
- Space weather and space physics research do not have to be expensive
- a laptop/desktop computer
- internet connection: CDAWeb provides free online database
  - Solar wind: OMNI
  - Geosynchronous orbit: GOES, LANL data
- Space weather forecast modeling with neural networks
  - HF backscatters from ionospheric irregularities (clutters)
  - Kp forecast models

Questions

- Could the next generation Palapa satellite provide magnetic field and other scientific data for space weather and space physics research?
- Could we use NN to predict spacecraft charging and other parameters at geosynchrnous orbit?


Thank you
2012 ISWI & MAGDAS